MSEG 410/610

Experimental Mechanics of Composite Materials

Lab 3: 0 and 90 Degree Compression Lab

Zachary Swain

Group Members

Chunyan Zhang

Evan Minnigh

Jerome Premkumar

Casey Busch

Performed on: March 13, 2019 Submitted on: March 22, 2019

Abstract

Objective:

The purpose of this lab was to predict and experimentally determine specific mechanical properties of a unidirectional carbon fiber laminate. This was done by executing experimental compressive loading of various specimens, as well as utilizing Rule of Mixtures (ROM) and a Self-consistent Field Model (CFM). This provided a better understanding of effective experimental compression testing, the mechanical properties that can be obtained from such experiments, and how to use and analyze different property prediction models.

Summary of Results:

Experimental compression testing of 0° and 90° oriented specimens from the fabricated unidirectional laminate resulted in moduli of E_1 = 11.66±0.22 Msi. and E_2 = 1.04±0.04 Msi, and fiber direction strength of X_1^C=91.68±5.53 ksi. The experimental results of E_2 line up very well with those of the CFM and ROM models, but experimental results for E_1 fall short of CFM and ROM results. This is attributed to the large relative standard deviation present for Fiber Volume Fraction (FVF), as well as the void content that was verified to be present in the laminate – both introducing inherent uncertainty in correlation between experimental and model-predicted results.

Procedure

ASTM Standard:

The panel was fabricated with a lay-up that will be described by nomenclature and notation as defined in ASTM D 6507. Compressive testing set up and operation was executed in accordance with ASTM D 3410.

Specimen Lay-up and Geometries:

The unidirectional laminate was fabricated with a $[0]_8$ lay-up[1] composed of G-83C resin and T700 carbon fiber prepreg.[2] Post-process machining was done to form two groups of perpendicular fiber orientation to produce specimens with geometries suitable for compresive testing.[3] A series of five 0° oriented test specimens and five 90° oriented test specimens were machined for compressive testing to examine the mechanical properties of the panel, compare the axial and transverse results, and to compare to multiple property prediction models. End tabs were machined to dimensions consistent with the pertaining ASTM, but two 0° specimens and one 90° specimen resulted in failure modes that are not acceptable for analysis. Three respective replacement specimens were made and tested in place of these failed specimens. Sampled and averaged specimen geometries for 0° and 90° testing can be found in Tables 1 and 2, respectively. Both specimen sets' samples were machined to 0.5 width by 0.15 inches, with specimen-specific nominal dimensions reported in Tables 1 and 2 (admissible by ASTM).

Instrumentation:

An Instron 5985 was used for compressive loading of each specimen. A Micro-Measurements strain gage of type CEA-06-125UE-350 was placed on each sample to record

axial and lateral strain data. The singular grid had a gage factor of 2.160±0.5% and transverse sensitivity of (+0.6±0.2)%; a resistance of 350.0±0.3% Ω with gage factor TC (+1.2±0.2) %/100°C. Bluehill and StrainSmart software suites were used to control and record data measurement. Microsoft Excel was utilized for data reduction purposes.

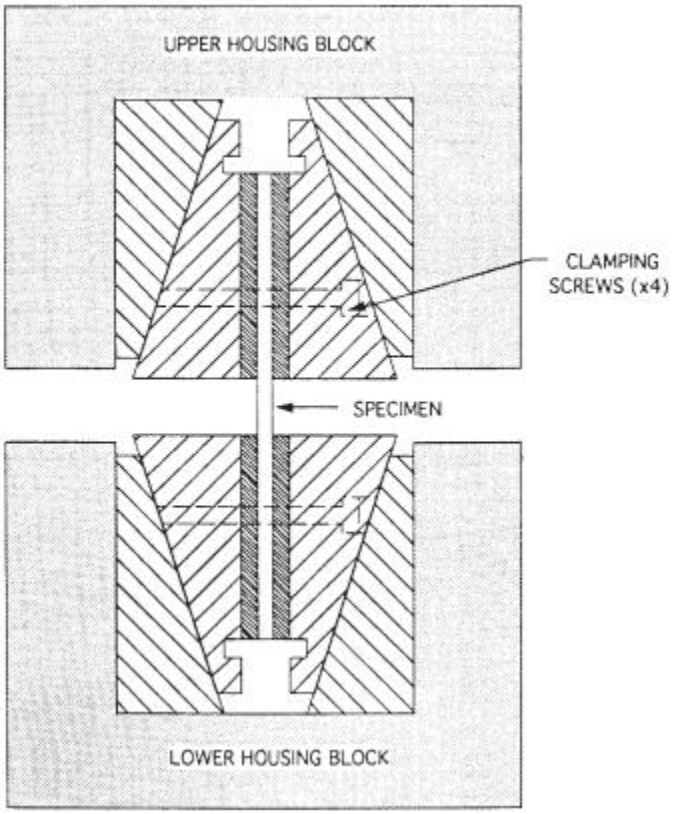

ASTM D 3410 housing diagram & specimen placement

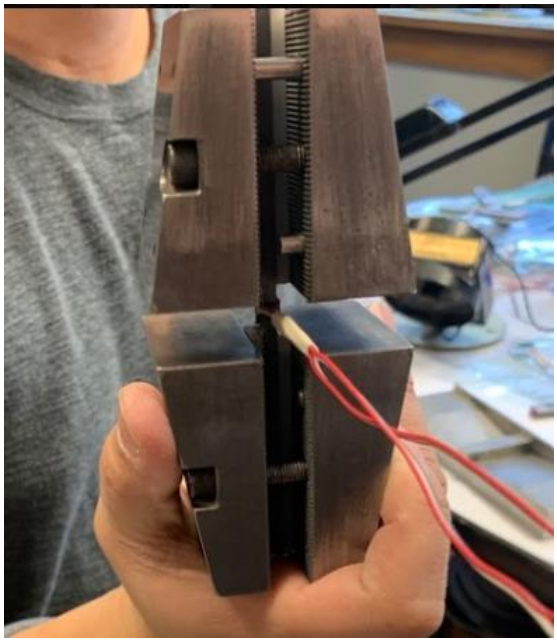

Experimental housing and specimen placement

Instron Settings:

Compression testing was operated with a 250kN (56000lb) load cell secured on the Instron 5985, and specimens were compressed at a 0.05 in/min crosshead rate. Instron input was modulated by the Bluehill software suite.

Testing Environment:

Testing was done in University of Delaware's Center for Composite Materials, inside a controlled test lab. Appropriate safety equipment was worn. Humidity levels were not closely monitored.

Results

Data Reduction Scheme:

Load and strain data obtained for each specimen tested were recorded and exported to excel. This data, in parallel with geometry specifications, were used to generate stress-strain curves, compliant with ASTM D3410, to characterize the mechanical properties of the specimen. The results were averaged over the 0° and 90° sample sets, and standard deviations were then calculated and reported. The resulting properties were compared to those resulting from ROM and CFM models and then analyzed.

Tables:

Specimen	**0° #1**	**0° #2**	**0° #3**	**0° #4**	**0° #7**
Width (in)	0.4965	0.4985	0.501	0.508	0.5
Thickness (in)	0.14255	0.14465	0.14915	0.1519	0.15535

Table 1: 0° specimen geometries

Specimen	**90° #2**	**90° #3**	**90° #4**	**90° #5**	**90° #6**
Width (in)	0.498	0.492	0.4915	0.497	0.4955
Thickness (in)	0.14595	0.1487	0.1508	0.1539	0.15265

Table 2: 90° specimen geometries

	#1					#2					#3		
	stress	avg strain	% bend			stress	avg strain	% bend			stress	avg strain	% bend
lower	23779.25	0.002001	0.025025		lower	11247.02	0.000999	0.025025		lower	10719.45	0.001001	0.082917
mid	35605.29	0.003	0.063		mid	22743.66	0.001999	0.01951		mid	21880.52	0.002002	0.028971
upper	47431.33	0.004	0.009997		upper	34309.65	0.003001	0.009997		upper	33443.07	0.003003	0.000333
end	93435.63	0.008098	0.001482		end	92389.19	0.008096	0.014514		end	83922.17	0.007349	0.039461
mod	11831959				mod	11519794				mod	11350461		

	#4				#7		
	stress	avg strain	% bend		stress	avg strain	% bend
lower	11831.79	0.001004	0.082669	lower	13118.76	0.001069	0.095416
mid	23456.23	0.001997	0.041562	mid	24383.65	0.002007	0.062048
upper	35106.59	0.002998	0.029191	upper	36060.51	0.002998	0.069224
end	72182.98	0.006222	0.017279	end	96968.14	0.008149	0.02577
mod	11675345			mod	11896160		

Table 3: 0° specimen results

	#2					#3					#4		
	stress	avg strain	% bend			stress	avg strain	% bend			stress	avg strain	% bend
lower	3109.393	0.002997	0.088603		lower	1052.488	0.001002	0.038442		lower	5167.436	0.005022	0.089008
mid	4182.546	0.004009	0.053511		mid	2227.993	0.002001	0.052237		mid	6206.32	0.006014	0.078317
upper	5104.357	0.005012	0.037613		upper	3253.144	0.003003	0.047619		upper	7285.68	0.006999	0.071296
end	24847.63	0.043752	0.208004		end	25669.76	0.052059	0.247777		end	25297.5	0.054623	0.303089
mod	990056.8				mod	1099503				mod	1071444		

	#5				#6		
	stress	avg strain	% bend		stress	avg strain	% bend
lower	967.472	0.001018	0.040275	lower	5261.905	0.005018	0.083499
mid	1948.018	0.002025	0.020005	mid	6240.25	0.006001	0.069244
upper	2980.86	0.002997	0.014851	upper	7324.361	0.007004	0.060822
end	24847.63	0.043752	0.208004	end	24035.54	0.045561	0.186212
mod	1017633			mod	1038497		

Table 4: 90° specimen results

Graphs of Stress-Strain Data:

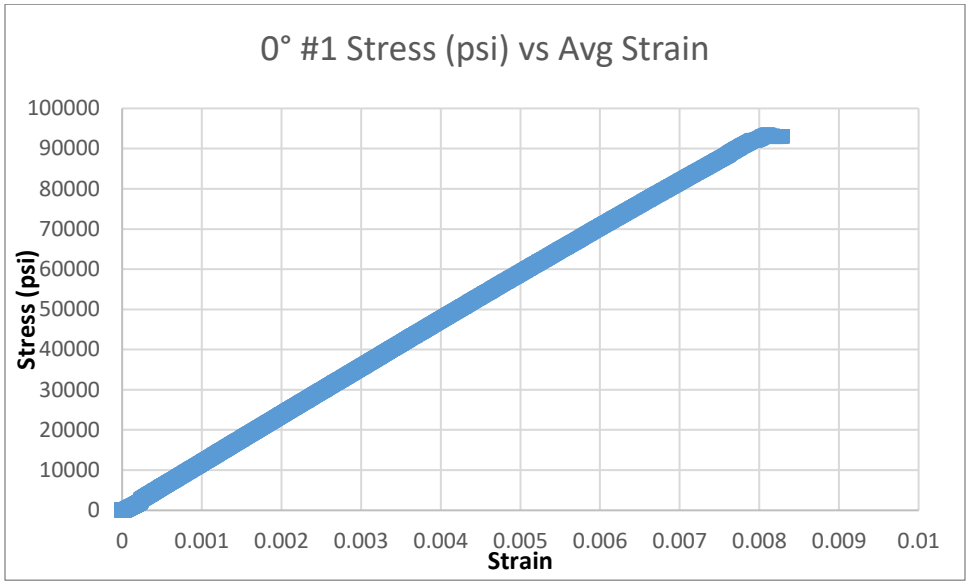

Fig. 1: 0° #1 stress-strain data

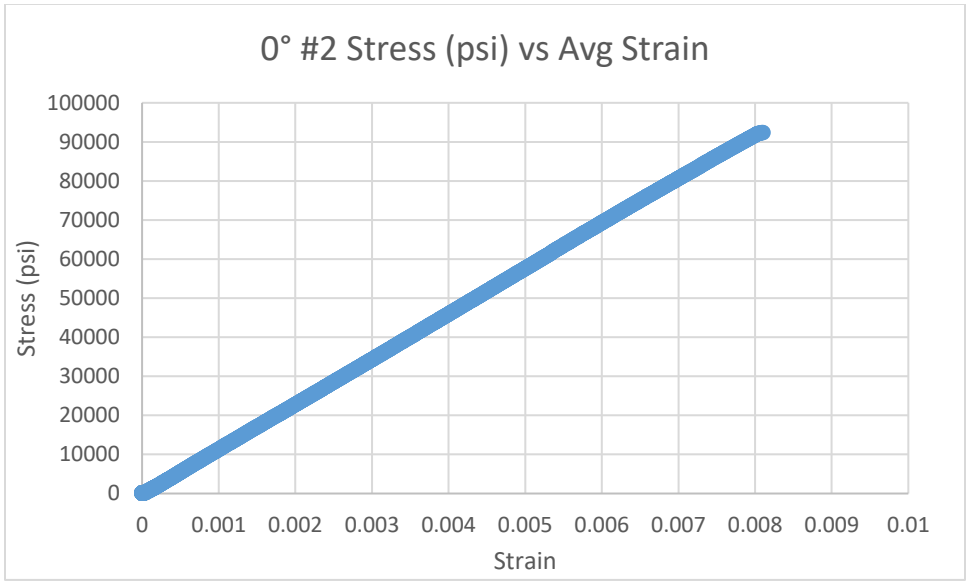

Fig. 2: 0° #2 stress-strain data

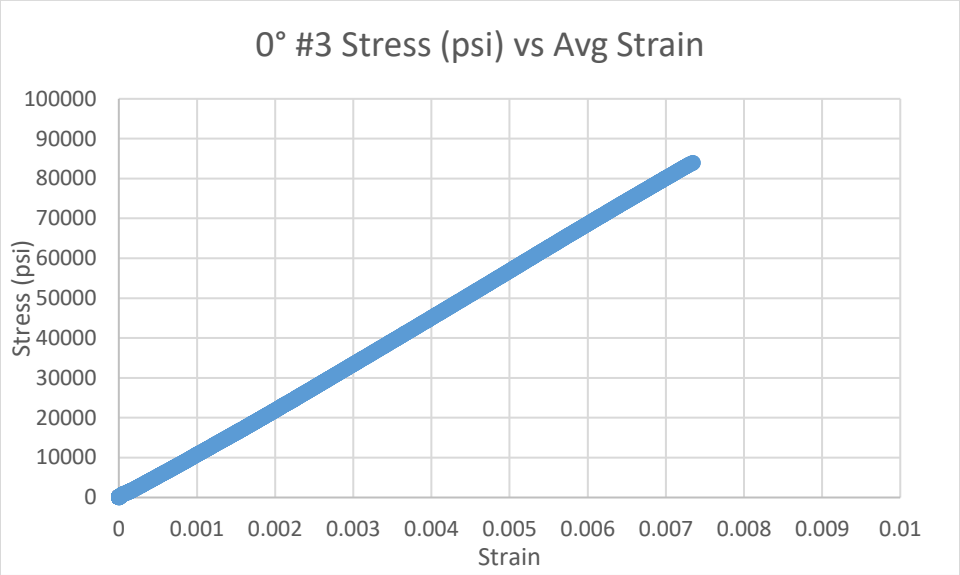

Fig. 3: 0° #3 stress-strain data

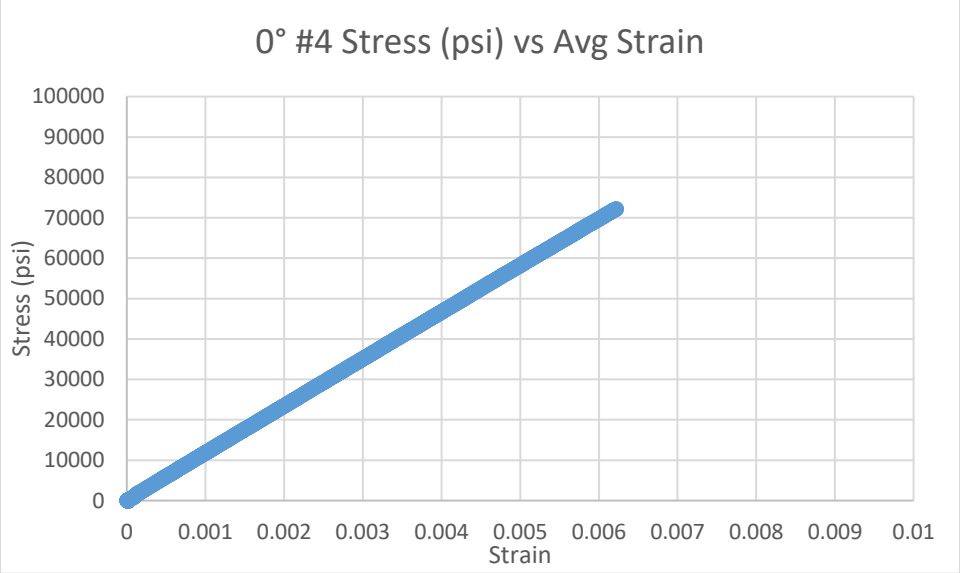

Fig. 4: 0° #4 stress-strain data

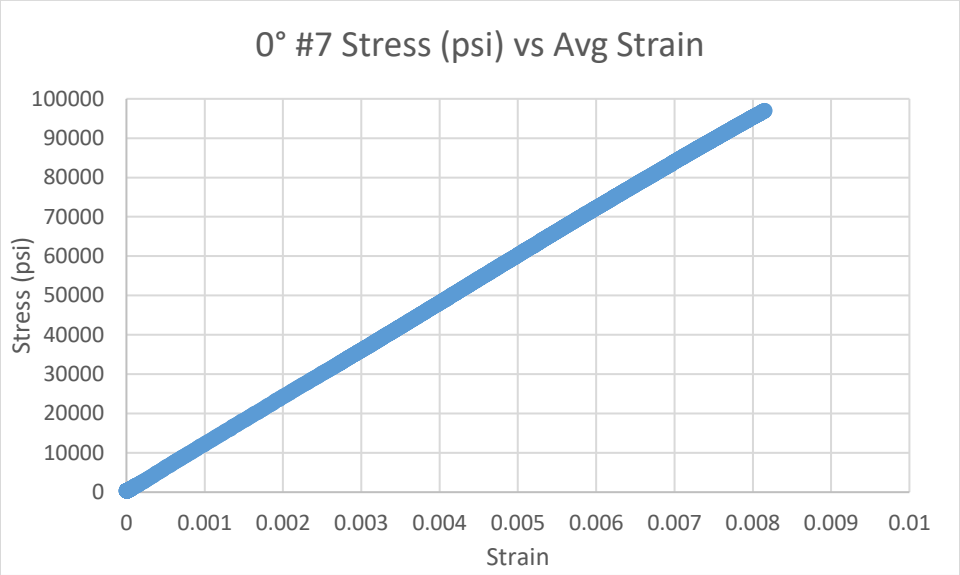

Fig. 5: 0° #7 stress-strain data

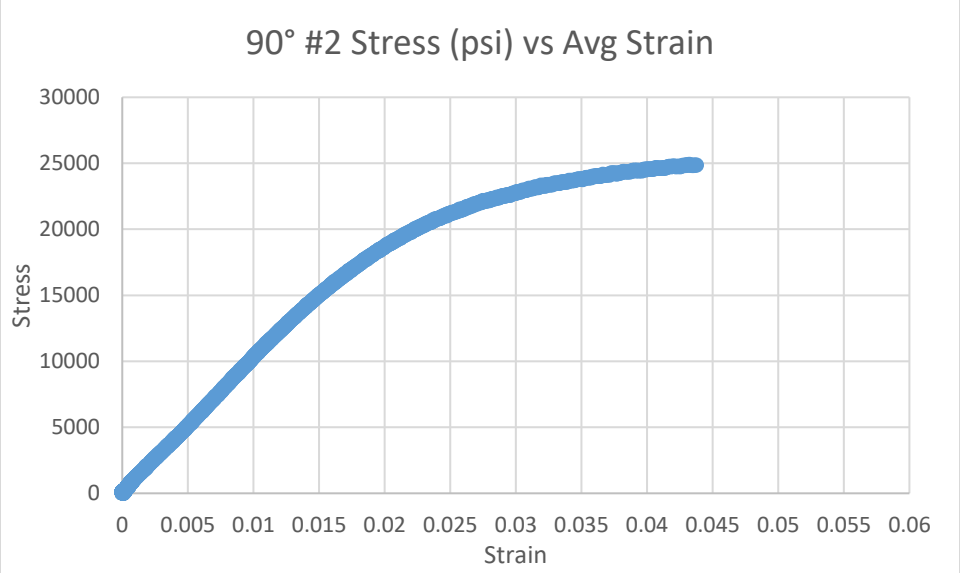

Fig. 6: 90° #2 stress-strain data

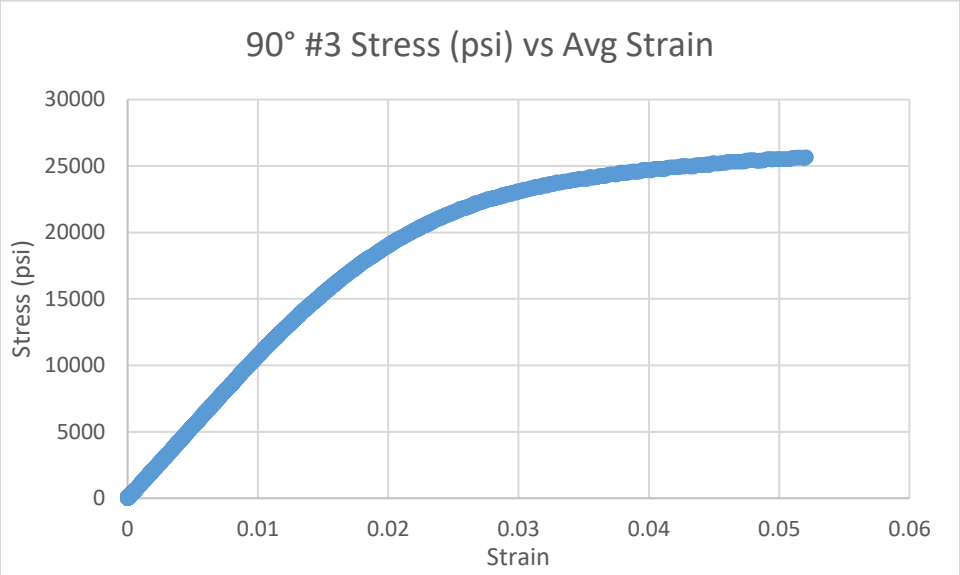

Fig. 7: 90° #3 stress-strain data

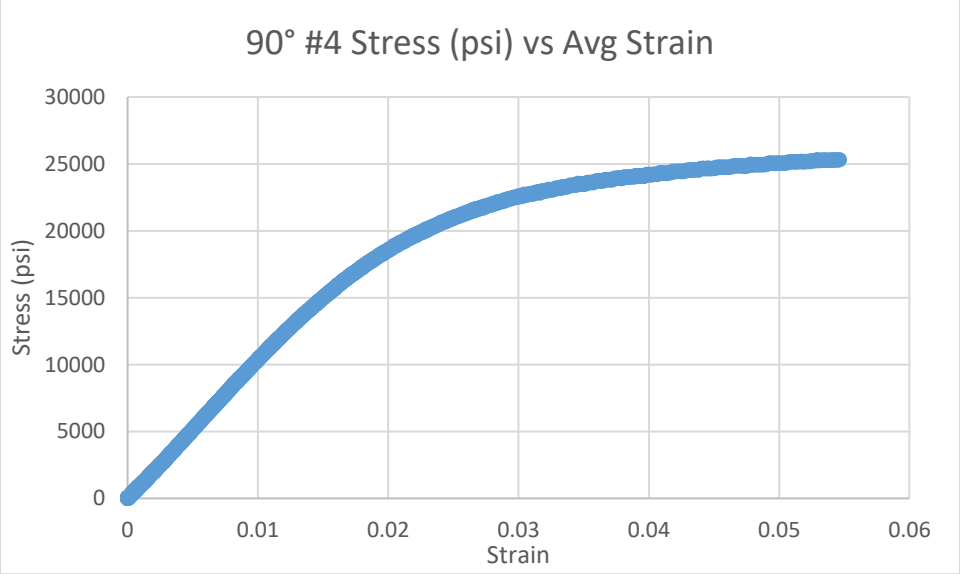

Fig. 8: 90° #4 stress-strain data

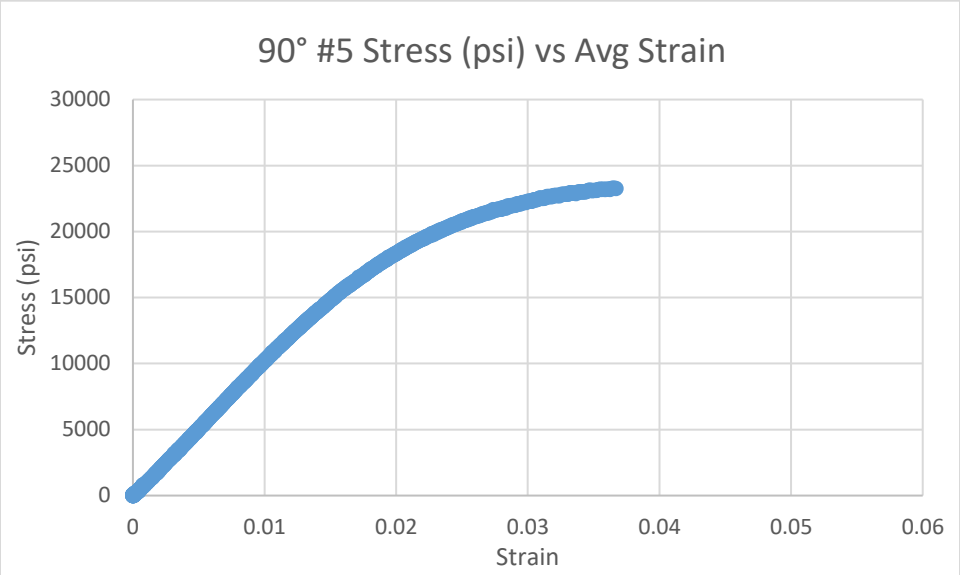

Fig. 9: 90° #5 stress-strain data

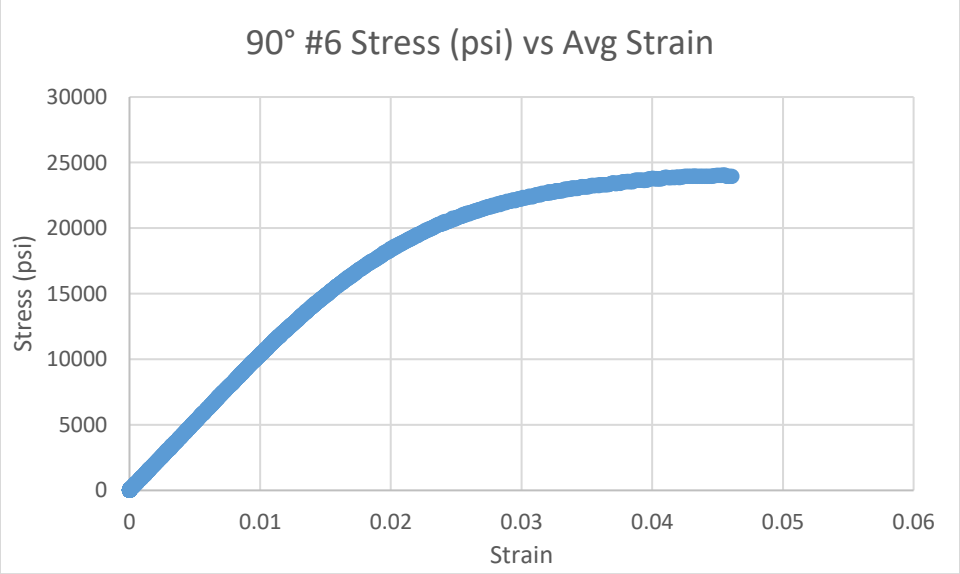

Fig. 10: 90° #6 stress-strain data

Summary of Test Results:

The specimens' cross-sectional area was first calculated by multiplying the averaged, sampled widths and thicknesses of each test bar. Each step of the recorded loading and stress data were imported into excel to be suitably manipulated. Each loading step was then divided by the specimen-specific cross-sectional area to obtain the stress generated at each step. The given μStrains from the recorded strain data were then converted to Strain for each step. Plots were generated relating the Stress (load/area) to the Strain of each recorded step for both specimen fiber orientations (Figs. 1-10). The 0° specimens averaged an ultimate compressive strength of 87779.62± 9947.39 psi. at an average ultimate strain of 0.00758± 0.00083. The 90° specimens experienced an average ultimate compressive strength of 24939.61± 611.45 psi. that caused an average ultimate strain of 0.0479±0.00506 ksi. in the samples.

Next, a strain region was defined - as specified in ASTM D 3410[3] - for each tested specimen, and Young's modulus of elasticity was determined over this strain range. It is important to note that for the 0° specimens, the specimens all failed over the applicable 0.006 strain threshold, while all of the 90° specimens fell short. The 90° specimens therefore had to be evaluated at an alternative appropriate strain range. When a specimen fails at an ultimate strain below 0.006, the ASTM standard generally recommends placing your strain region at 25% and 50% of the ultimate strain experienced. However, all 90° specimens experience significant plastic deformation prior to reaching 50% of their ultimate strain. This would certainly impact the calculated modulus of elasticity, and can be visualized in the yield stresses found by 0.002 strain offset shown in Figs. 11-15. So an applicable strain range is found above the low-load buckling region (Degree of Bending <0.1), but before reaching significant yield (0.002 strain offset). These strain regions are reported above in Table 4, labeled as "lower" and "upper" bounds of the strain region. Other

designations “mid” and “end” respectively refer to the middle strain point between the two bounds and to the ultimate strain seen before failure. It is likewise important to assess the degree of bending found at the midpoint of the chosen strain region, to ensure buckling effects remain insignificant over the entire region; all specimens are found to pass this stipulation. The data represented in Tables 3 and 4 are largely represented in summarized Tables 5 and 6, respectively. Degree of bending is calculated as

$$(\varepsilon_1 - \varepsilon_2)/(\varepsilon_1 + \varepsilon_2)$$

and is represented as “% bend” in tables 3 and 4. This degree of bending is inspected to ensure the specimen is not experiencing any excessive buckling.

If bending exceeds 0.1 in the strain region in question, buckling effects are no longer considered to be negligible, and it can no longer be considered to provide valid or meaningful results as per the ASTM.[3] If this value does exceed 0.1, it cannot be said to truly isolate the compressive properties of the material. As such, properties must be evaluated over a strain region where Degree of Bending < 0.1. Degree of bending for each sample is shown in Figs. 24-33 in Appendix A. Experimentally, buckling is seen in a divergence in strain, as measured by the back-to-back strain gages. Opposing compressive and tensile strains in back-to-back strain gages are characteristic of significant buckling. Strain, by strain gage, is plotted for all specimens tested in Figs. 34-43 available in Appendix A.

	Averaged Value	s.d	%RSD
Ult. Strength (psi)	87779.62	9947.39	11.33
Modulus (Msi)	11.655	0.224	1.923
Ult. Strain	0.007583	0.00083	10.95

Table 5: 0° specimen averaged stress-strain results

	Averaged Value	s.d	%RSD
Ult. Strength (psi)	24939.61	611.449	2.451718
Modulus (Msi)	1.043	0.0432	4.140904
Ult. Strain	0.047949	0.005059	10.55048

Table 6: 90° specimen averaged stress-strain results

Since the 90° specimens did undergo significant plastic deformation, the yield stress can be calculated by simply utilizing a 0.002 strain offset. This offset-intercept yield stress is averaged over the 5 specimens and found to be 18204±1004.2 psi. The 0° orientation specimens are not seen to experience significant plastic deformation before failure, due to the stiffness imparted by the axial orientation of the fibers.

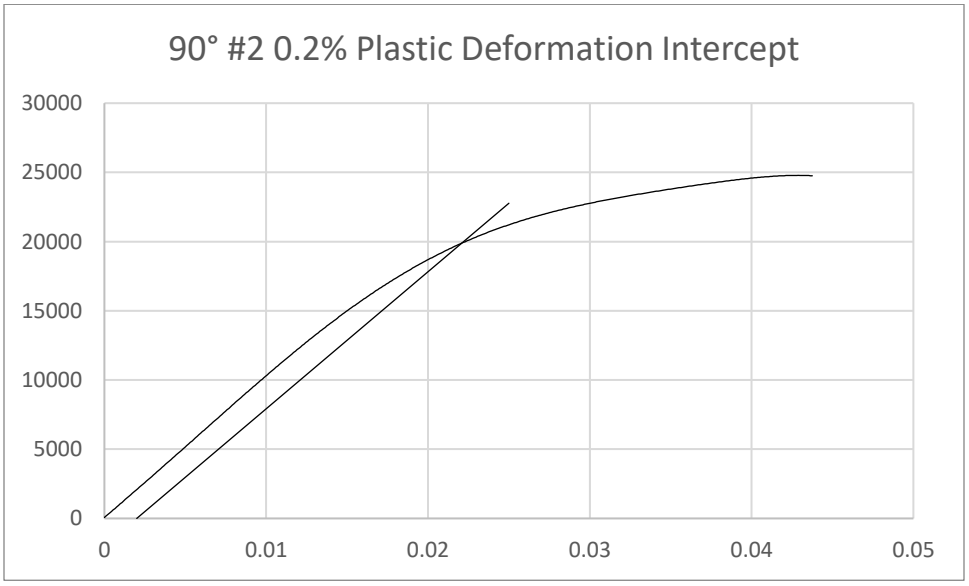

Fig. 11: 90° #2 stress-strain, 0.002 strain offset intercept

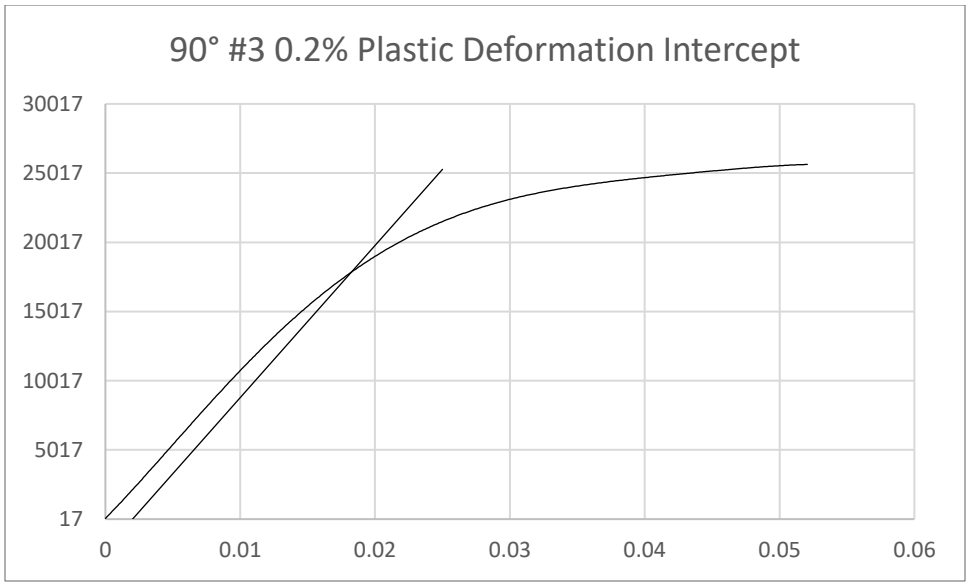

Fig. 12: 90° #3 stress-strain, 0.002 strain offset intercept

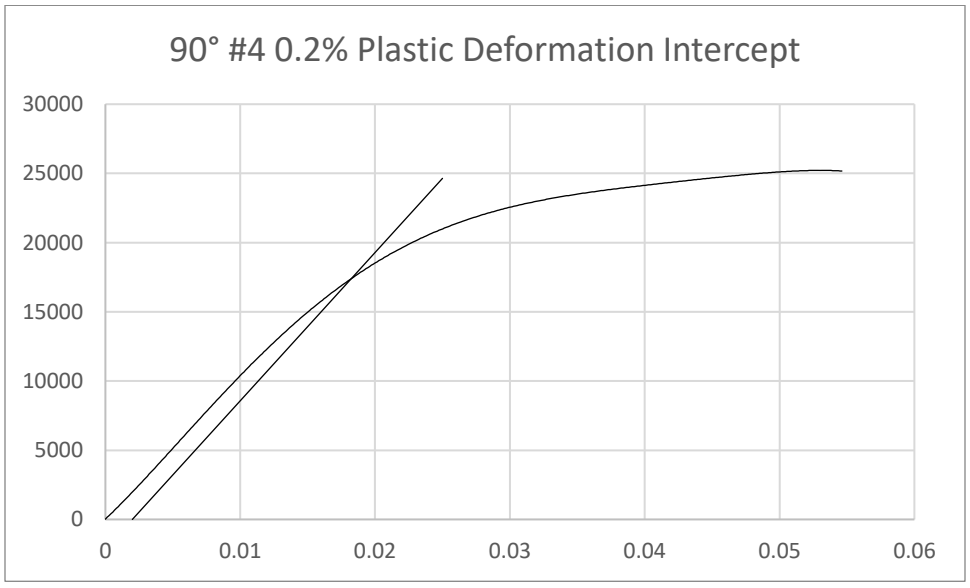

Fig. 13: 90° #4 stress-strain, 0.002 strain offset intercept

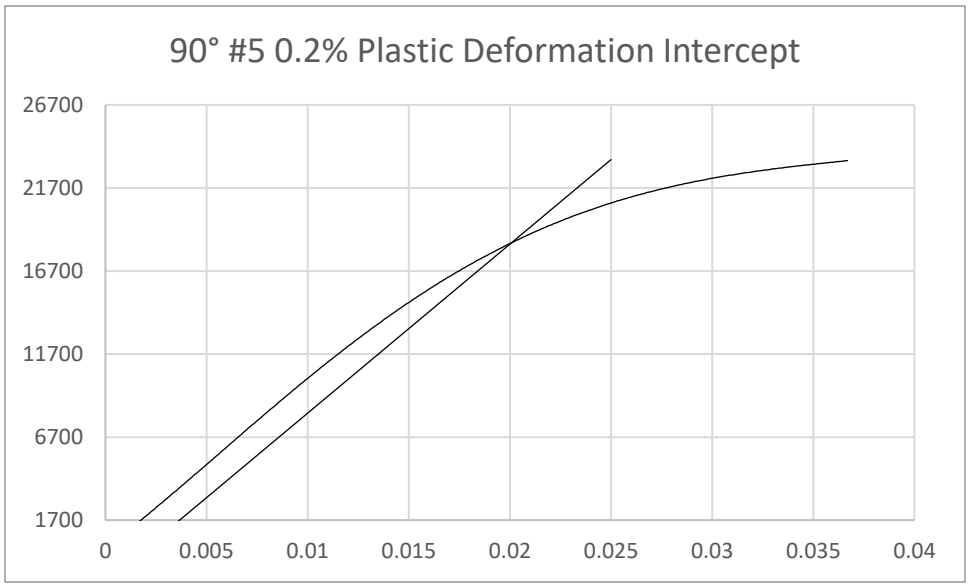

Fig. 14: 90° #5 stress-strain, 0.002 strain offset intercept

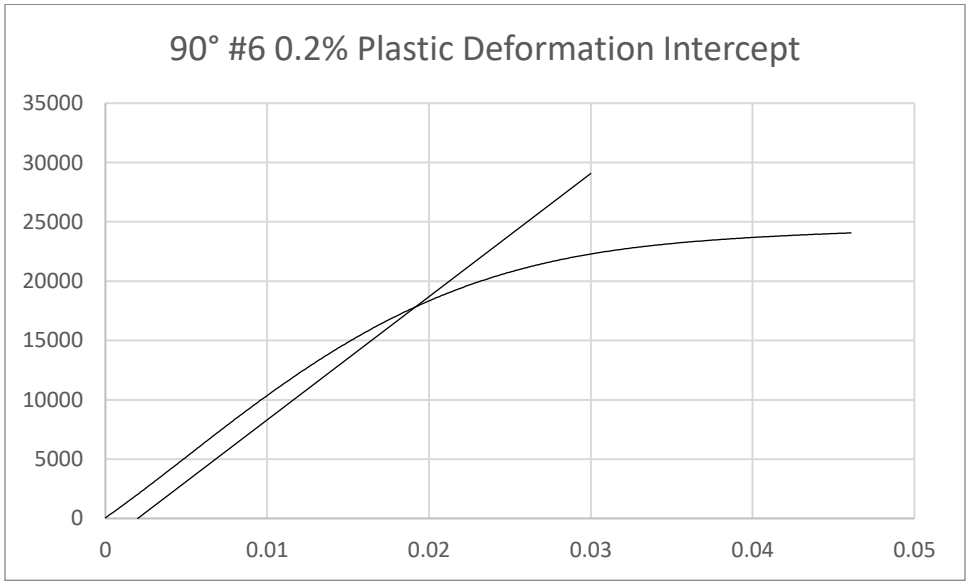

Fig. 15: 90° #6 stress-strain, 0.002 strain offset intercept

Sample #	2	3	4	5	6
Yield stress (psi)	19850	17700	17300	18420	17750
				Average	18204
				s.d.	1004.2

Table 7: 90° specimen yield stress results

Description of Failure Modes:

Images were recorded of each sample after it had undergone compressive testing and ultimate failure. Figs. 16 and 17 show the 0° specimens from two separate angles, while Figs. 18 and 19 display that of the 90° samples.

Fig. 16: 0° failed samples

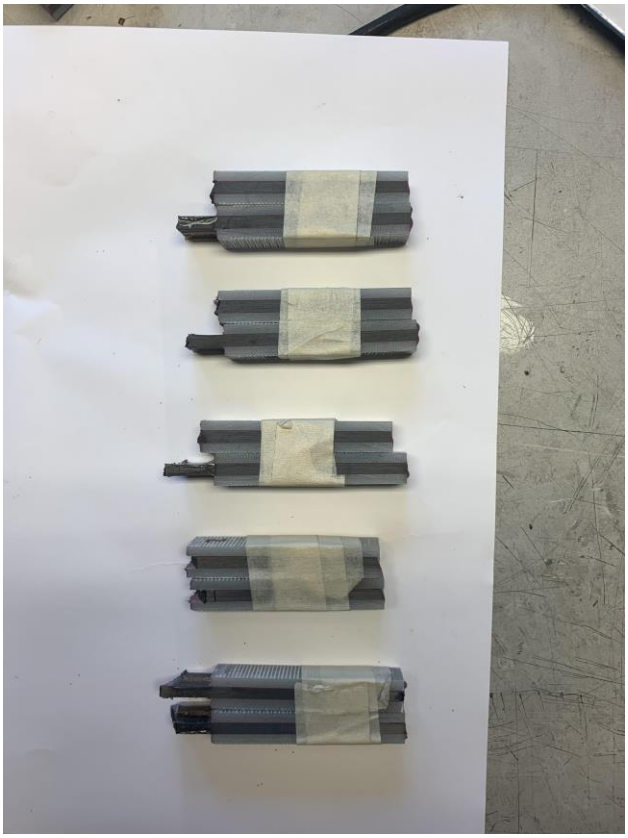

Fig. 17: 0° failed samples (side)

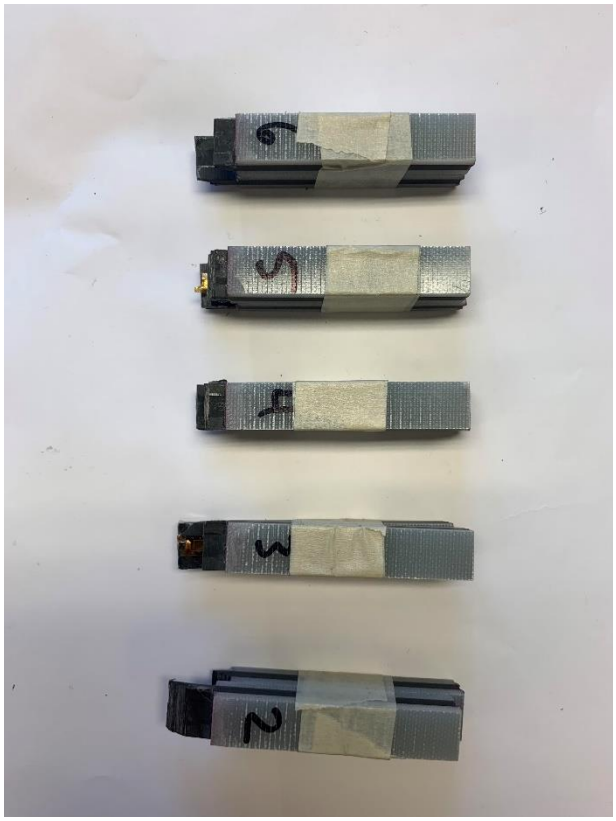

Fig. 18: 90° failed samples

Fig. 19: 90° failed samples (side)

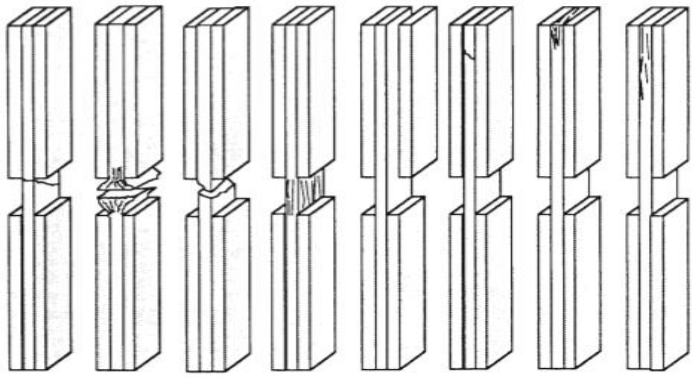

TAT BGM HAT SGV Acceptable Failure Modes and Areas

DTT HIT CIT DIT Unaceptable Failure Modes and Areas

First Character

Failure Mode	Code
Angled	A
Brooming	B
end-Crushing	C
Delamination	D
Euler buckling	E
tHrough-thickness	H
Kink bands	K
Lateral	L
Multi-mode	M(xyz)
long.-Splitting	S
Transverse shear	T
eXplosive	X
Other	O

Second Character

Failure Area	Code
Inside grip/tab	I
At grip/tab	A
Gage	G
Multiple Areas	M
Tab adhesive	T
Various	V
Unknown	U

Third Character

Failure Location	Code
Bottom	B
Top	T
Left	L
Right	R
Middle	M
Various	V
Unknown	U

Fig. 20: ASTM D 3410 compressive failure mode specifications[3]

From the 0° fiber-oriented sample set, specimens 1 and 2 are seen to have experienced TAT failure, as defined in Fig. 19. It is determined that the 1 and 2 samples were grouped incorrectly for the pictures, both tops being paired as "2" and bottoms as unlabeled "1." Specimens 3, 4, and 7 were determined to have experienced LAB failures. For the 90° specimen set, 2 is seen to have HAB failure, while 3, 4, and 6 all experienced HAT failure modes. 4 seems to have a somewhat-reserved BGM failure mode. All analyzed failure modes are determined to be acceptable as per the ASTM standard's specifications.

Error Analysis

The relevant values for error analysis are given in Table 8, below.

Value	Ave.	s.d.
E_1 (Msi)	11.655	0.224
E_2 (Msi)	1.043	0.0432
0° Ult. Strength (Msi)	87.78	9.947
90° Ult. Strength (Msi)	24.94	6.115
Yield stress (ksi)	18.204	1.004
FVF	0.539	0.06

Table 8

All values are found to have a percent relative standard deviation (%RSD) within ~4%, with the exception of Ultimate Strains for both specimen sets, 0° Ultimate Strength, and Fiber Volume Fraction; these properties were found to have %RSD ~10%. The deviating FVF will be accepted, as the averaging of FVF is obtained from all results of Lab Report 1, and there is no other way to obtain better sampled results at present. Significant variation in Ultimate Strain has ben seen across the board in all experimental testing conducted as a part of this course, without necessarily directly impacting the variability in tensile or compressive moduli. As such, this variation will be

hesitantly accepted. The large variability in 0° Ultimate Strength does give pause, however. The driving force causing this averaged value to have such a relatively large standard deviation is specimen #4, which can be seen to have a much lower Ultimate Strength than any other samples, despite having a undeviating modulus. Specimen #4 will be considered an outlier in this analysis, and eliminating #4 from averaging, 0° Ultimate Strength will be calculated to be 0.09168±0.00553 Msi, halving the standard deviation.

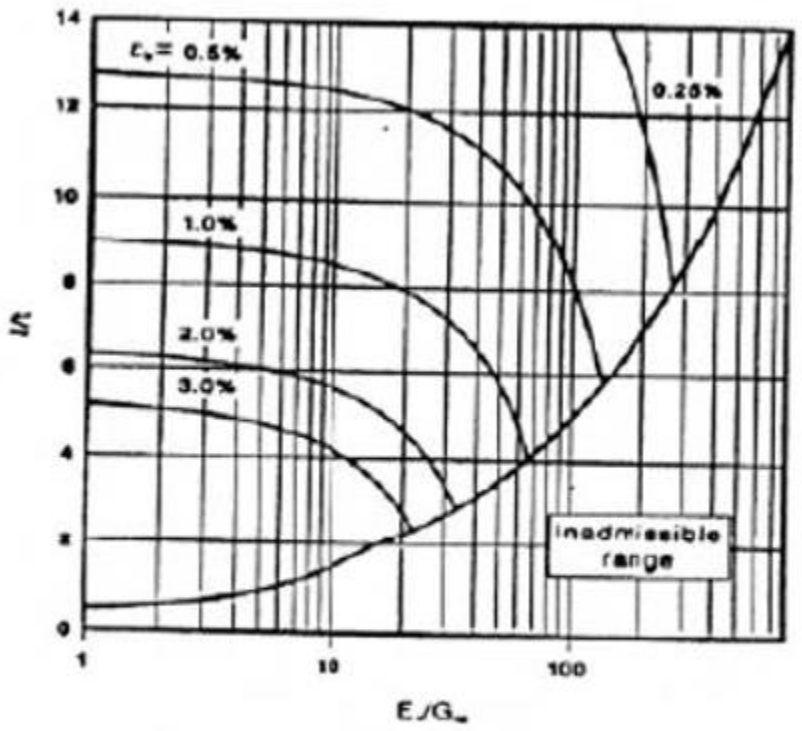

Figure (8) : Specimen Design for Accurate Modulus Determination and Strength Measurement

From the results reported in Tables 5, 6, 8, and the above diagram, specimen dimensions can be designed for gage length to thickness ratio. E/G is approximated by E_1^C/G_M , with experimental and manufacturer data.

$$E_1^C/G_M = (11.655E6)/(487E3) = 23.9$$

Ultimate strain is then taken at its mean reported experimental values of 0.76% for 0° fiber orientation compression testing, and 4.8% for 90° orientation (Tables 5 and 6). It is important to note that these reported values have significant standard deviation relative to their magnitude, and may not be precisely reliable; this dimensioning analysis is meant as an approximation, and can be more closely examined in future works. For 0° oriented specimens, the diagram above relates a 23.9 E/G at 0.76% ε_u to a recommended l/t approximated as 9.5. For the 0.15" thickness used, a 1.425 length gage section is recommended by a 9.5 l/t ratio for 0° oriented compression samples. For 90° oriented specimens with 23.9 E/G at 4.8% ε_u, l/t falls in the inadmissible range with such a high ε_u. Should the ε_u vary to the admissible range threshold of ~2.8% for 23.9 E/G, the resulting l/t would be approximately 2.5. For the 0.15" thickness used, a 3.75 length gage section is recommended by a 2.5 l/t ratio for 90° oriented compression samples with 2.8% ε_u.

Theoretical Predictions

Theoretical predictions using the Rule of Mixtures and Self-consistent Field Model are provided in Appendix B.

Correlation of Theory and Experiments

Method	value	range low	range high	units
	E1	11.44	11.88	Msi
experiment	E2	1.00	1.08	Msi
	X_1c	86.15	97.21	ksi
	E1	16.25	20.2	Msi
ROM	E2	0.9347	1.214	Msi
	X_1c	345.94	449.47	ksi
	E1	16.25	20.2	Msi
CFM	E2	0.721	1.235	Msi

Table 9: Summary of all methods' results

The result of ROM and CFM E_1 predictions match each other quite well due to the high degree of accuracy of the ROM for E_1. Their values don't, however, align with those measured experimentally for E_1. The lower experimental compressive modulus result is attributed to laminate defects known to be in the panel, as reported in Lab 1, as well as compressive moduli being known to manifest in artificially low results in experimental testing. The void content in the panel is above 1% and cannot be used in certain application due to its lesser – and widely variable – mechanical properties.

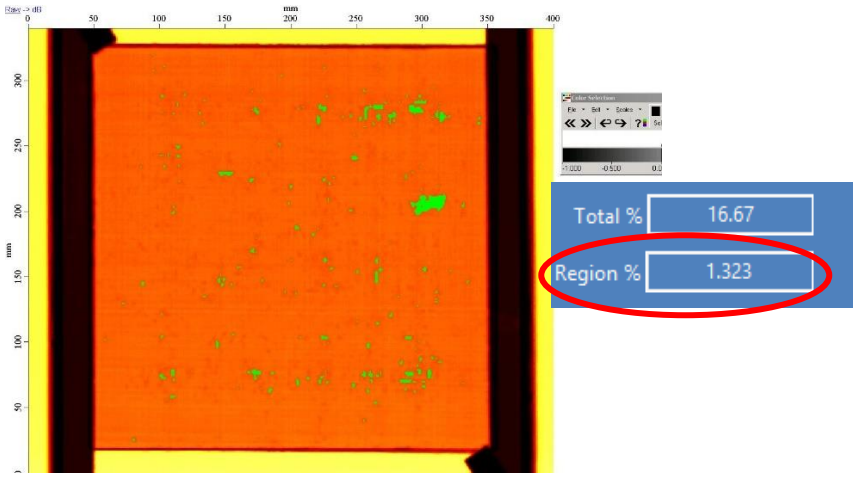

Fig. 21: C-scan results of panel.

The experimental results for E_2, 90° compressive stiffness, fall well within the range of ROM and CFM predicted values. This is a promising result for the experimentally calculated lateral compressive modulus.

Conclusions

Experimental compression testing of 0° and 90° oriented unidirectional carbon fiber epoxy composite specimens from the fabricated laminate resulted in moduli of E_1 = 11.66±0.22 Msi. and E_2 = 1.04±0.04 Msi, as well as axial strength of X_1^C=91.68±5.53 ksi. The experimental results of E_2 line up very well with those of the CFM and ROM models, but experimental results for E_1 fall somewhat short of CFM and ROM results. This is attributed to the large relative standard deviation present for Fiber Volume Fraction (FVF), as well as the void content that was verified to be present in the laminate – both introducing inherent uncertainty in correlation between experimental and model-predicted results. Experimental strength results, however, fall significantly below the predicted value range. This is likely due to how the strength is being modelled in its predicted calculation. The shear modulus of the matrix is used in isolation from fiber and fiber-matrix-interface influences to predict the ultimate strength of the fiber-epoxy laminate. This results in an approximated prediction of compressive strength that far-exceeds the experimental results; predictions are ~4 times greater than the experimental values. This resultant disparity gives insight to limitations of predictive property approximates, and provided experience in how to skeptically analyze results of modelling and assumptions being made.

References

[1]] ASTM Standard D6507, 2016, “Standard Practice for Fiber Reinforcement Orientation Codes for Composite Materials,” ASTM International, West Conshohocken, PA, 2003, DOI: 10.1520/D6507-16, www.astm.org/Standards/D6507.htm.

[2] T700S Data Sheet [PDF]. Santa Ana, CA: Toray Carbon Fibers America Inc. https://www.toraycma.com/file_viewer.php?id=4459.

[3] ASTM Standard D3410, 2006, “Standard Test Method for Compressive Properties of Polymer Matrix Composite Materials with Unsupported Gage Section by Shear Loading,” ASTM International, West Conshohocken, PA, 2006, www.astm.org/Standards/D3410.htm.

[4] G-83C Data Sheet [PDF]. Santa Ana, CA: Toray Carbon Fibers America Inc. (Digital).

Appendix A

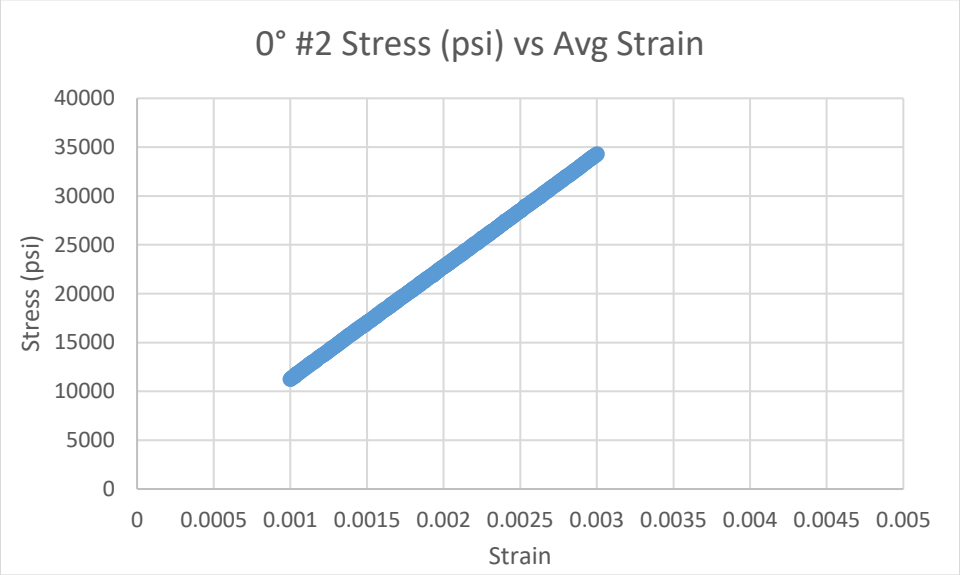

Fig. 22: Example strain range of E_1 for 0° #2.

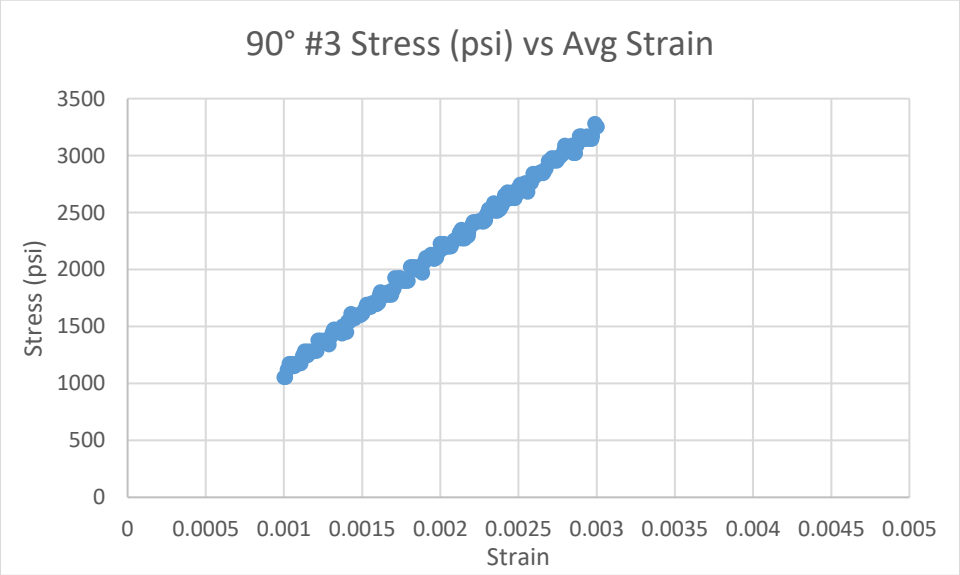

Fig. 23: Example strain range of E_2 for 90° #3.

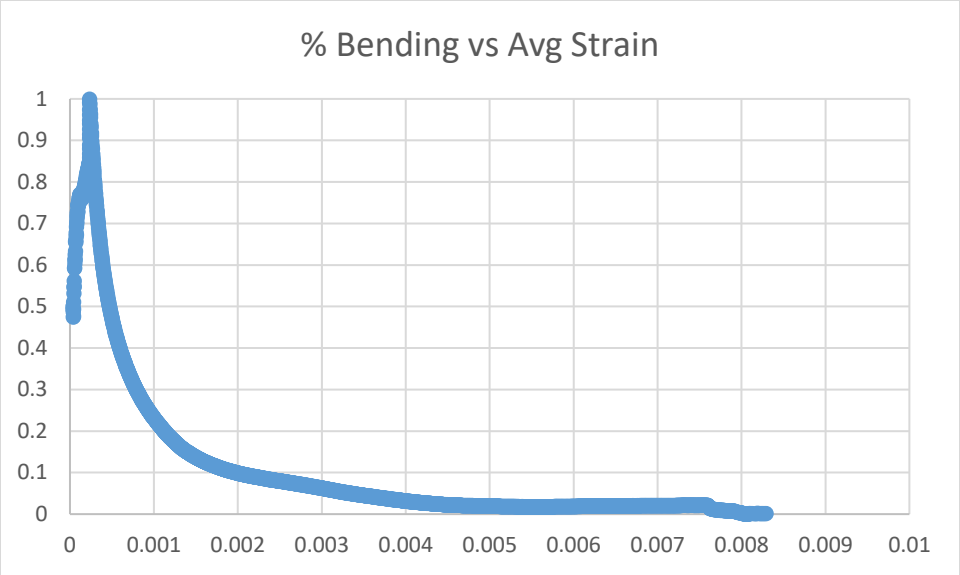

Fig. 24: % Bending as a function of Average Strain for 0° #1.

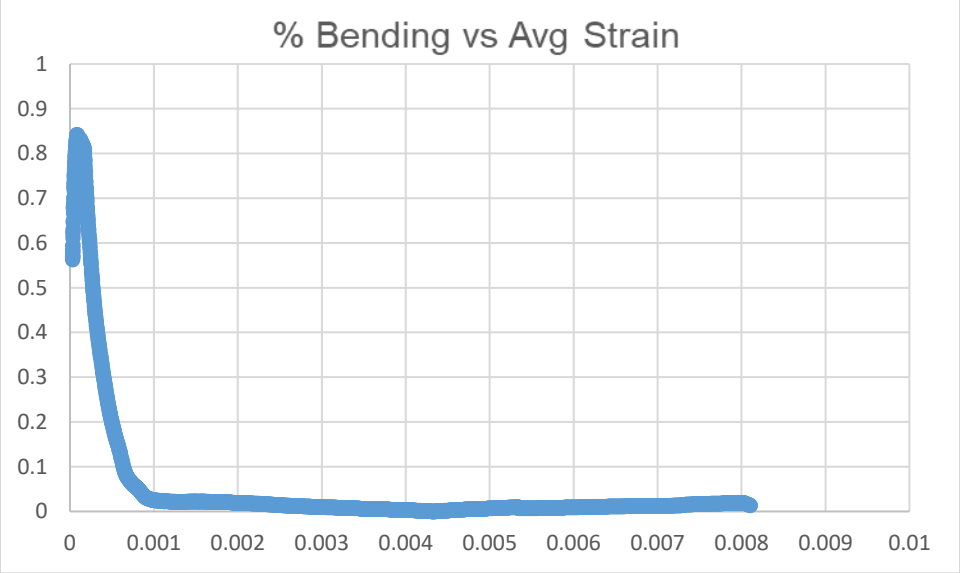

Fig. 25: % Bending as a function of Average Strain for 0° #2.

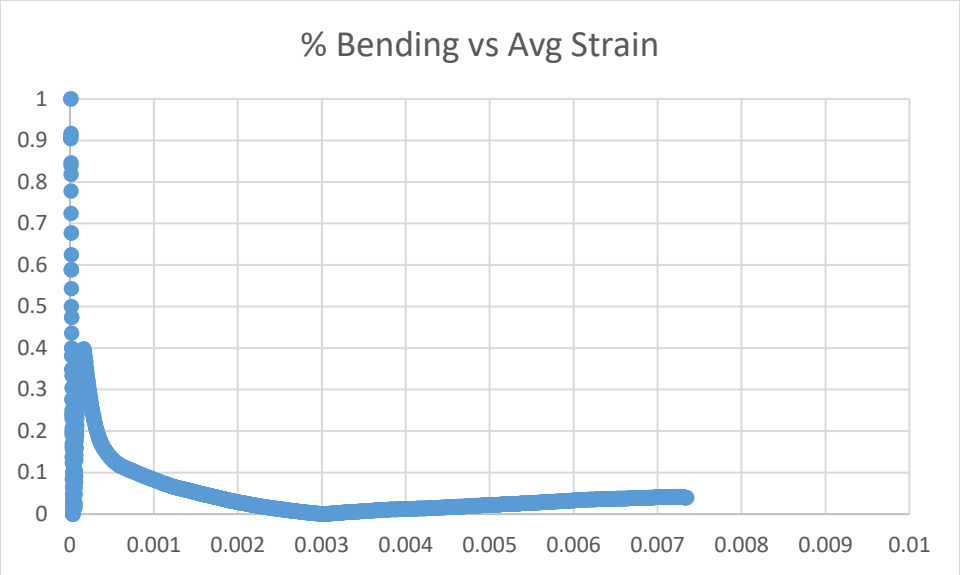

Fig. 26: % Bending as a function of Average Strain for 0° #3.

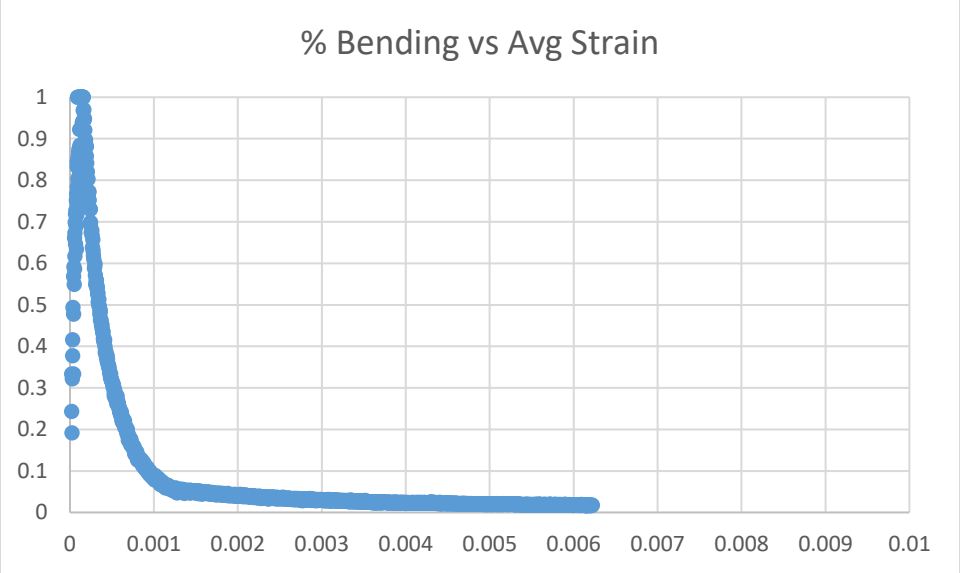

Fig. 27: % Bending as a function of Average Strain for 0° #4.

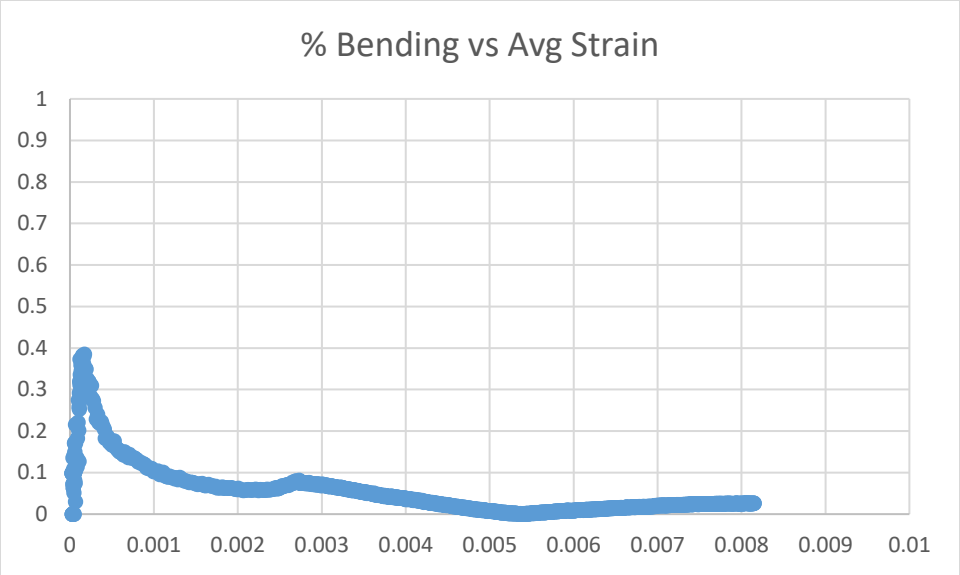

Fig. 28: % Bending as a function of Average Strain for 0° #7.

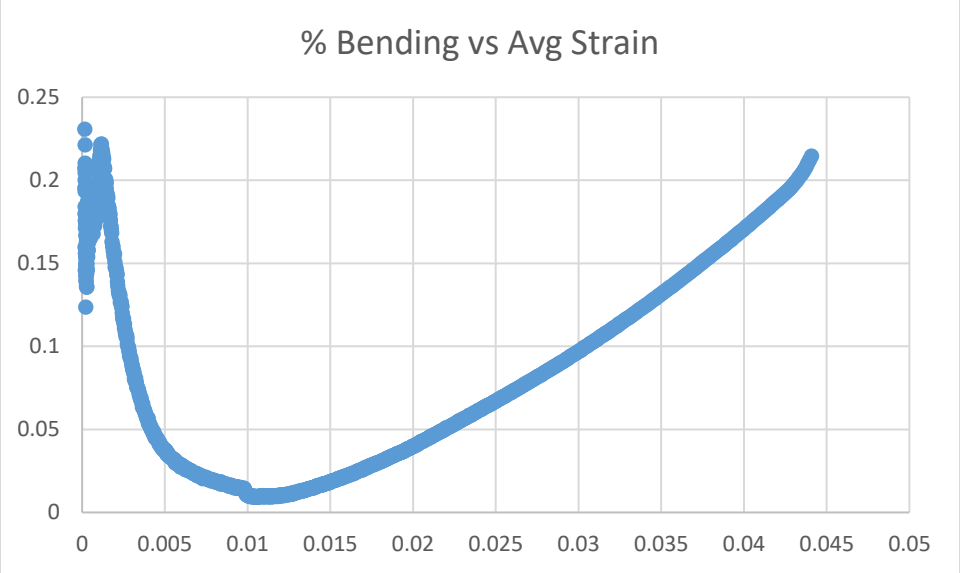

Fig. 29: % Bending as a function of Average Strain for 90° #2.

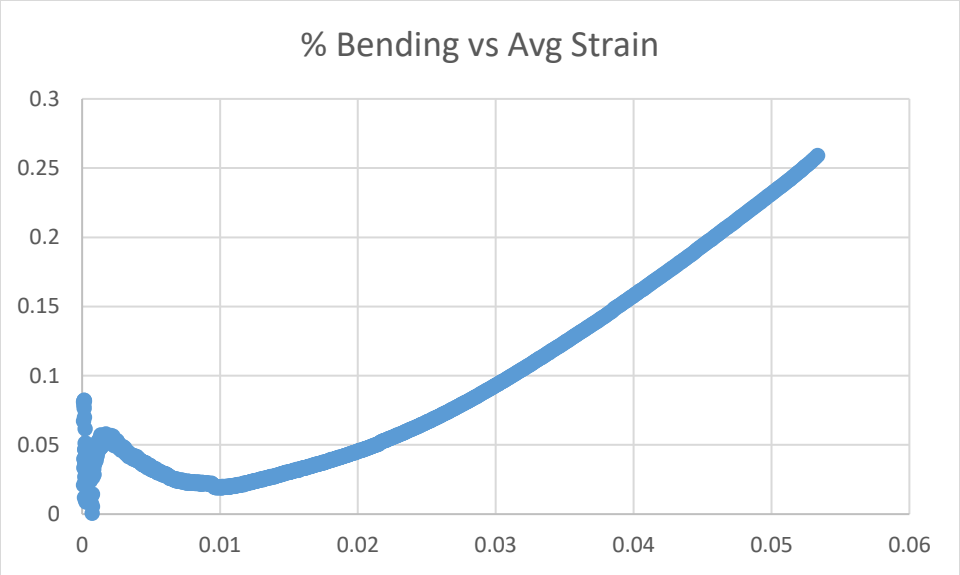

Fig. 30: % Bending as a function of Average Strain for 90° #3.

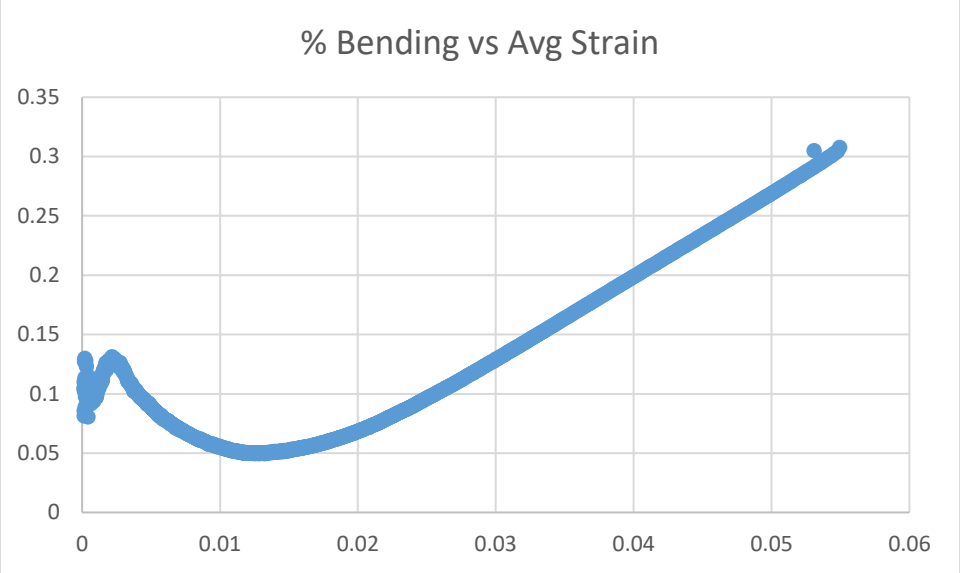

Fig. 31: % Bending as a function of Average Strain for 90° #4.

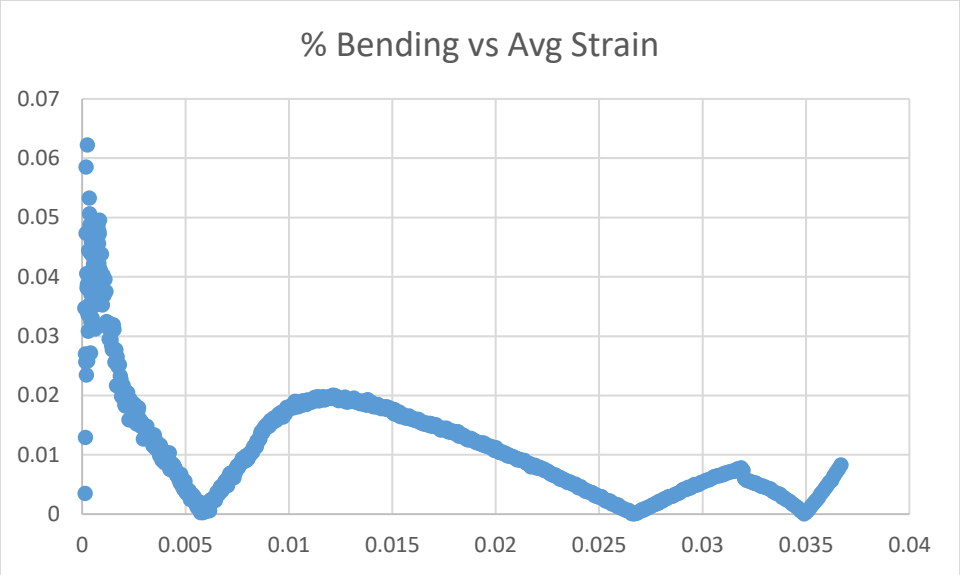

Fig. 32: % Bending as a function of Average Strain for 90° #5.

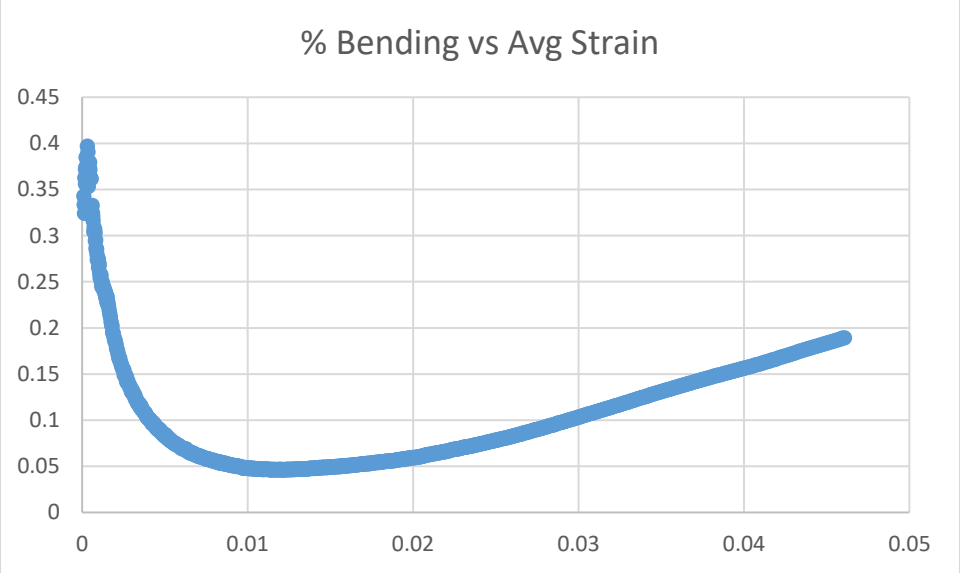

Fig. 33: % Bending as a function of Average Strain for 90° #6.

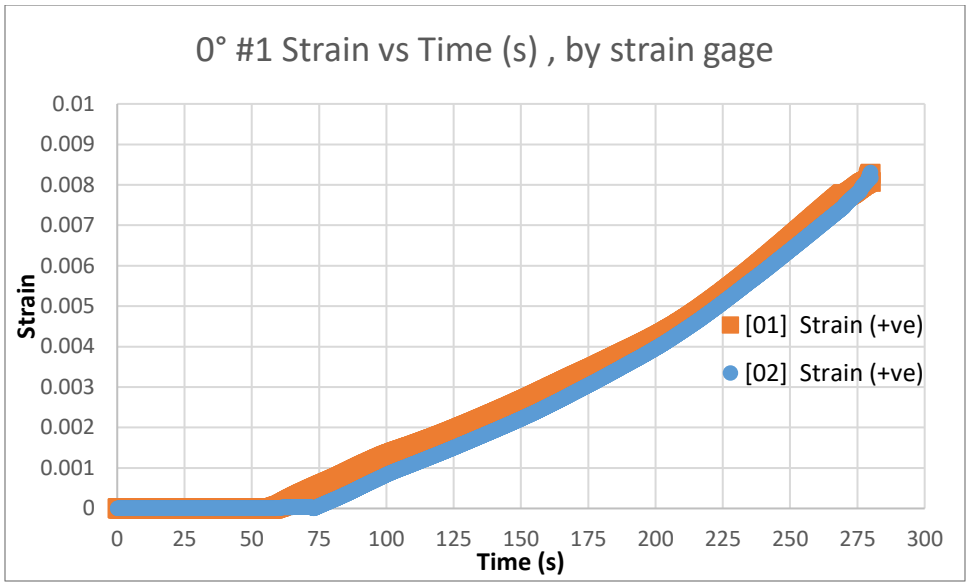

Fig. 34: Strain vs time interval sampling, by strain gage for 0° #1.

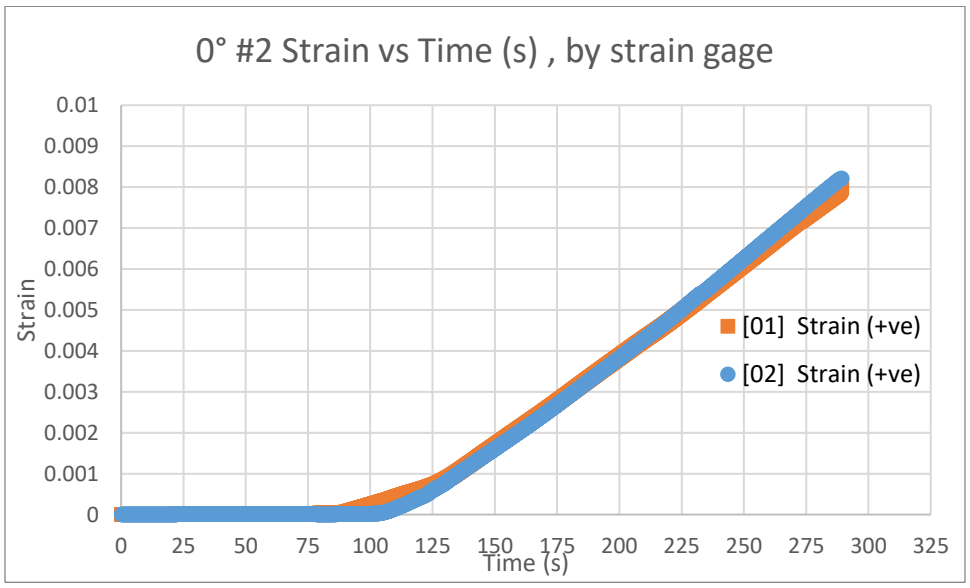

Fig. 35: Strain vs time interval sampling, by strain gage for 0° #2.

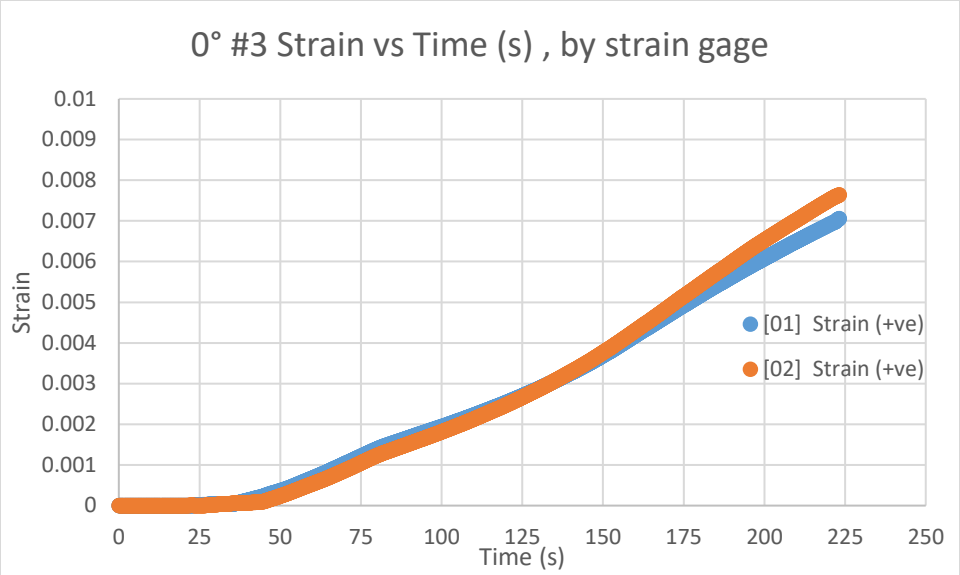

Fig. 36: Strain vs time interval sampling, by strain gage for 0° #3.

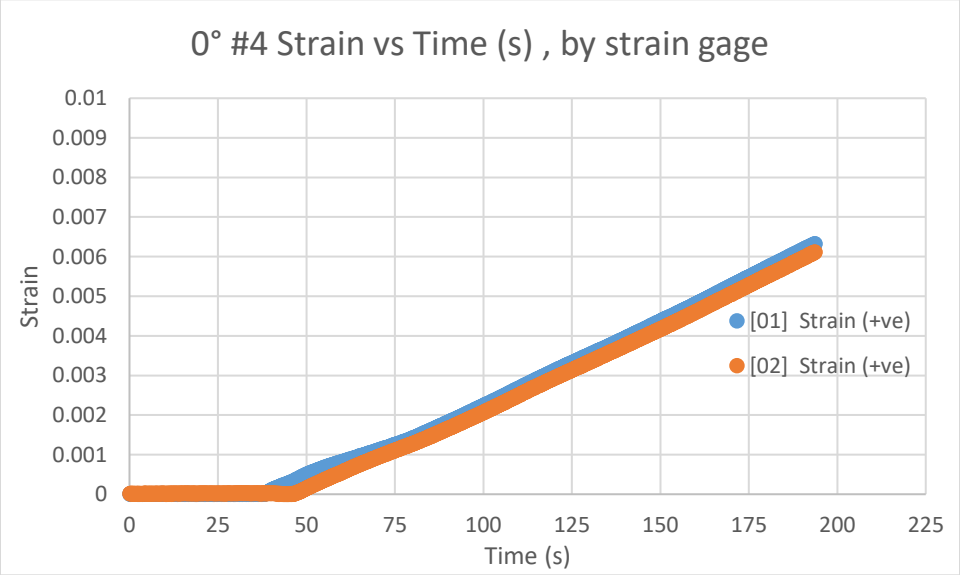

Fig. 37: Strain vs time interval sampling, by strain gage for 0° #4.

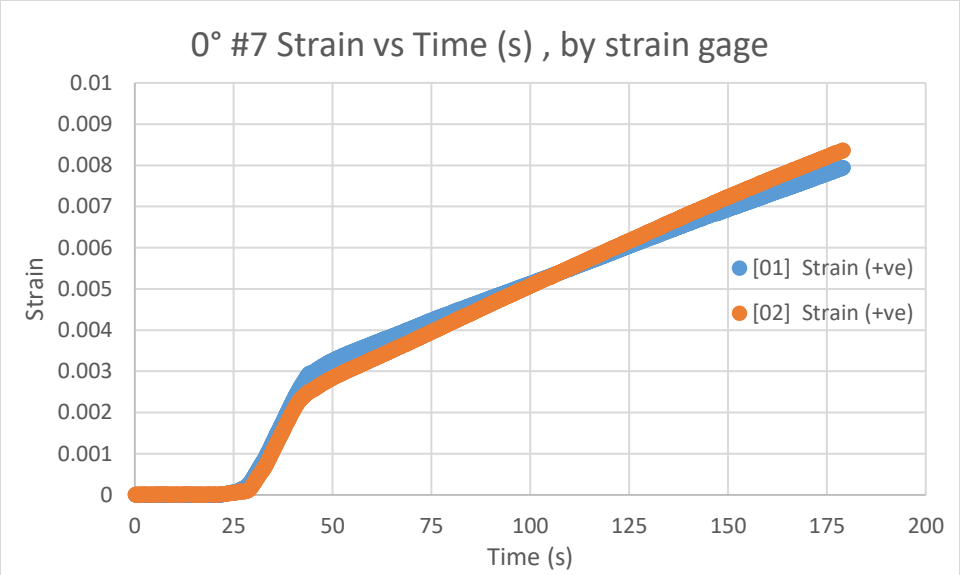

Fig. 38: Strain vs time interval sampling, by strain gage for 0° #7.

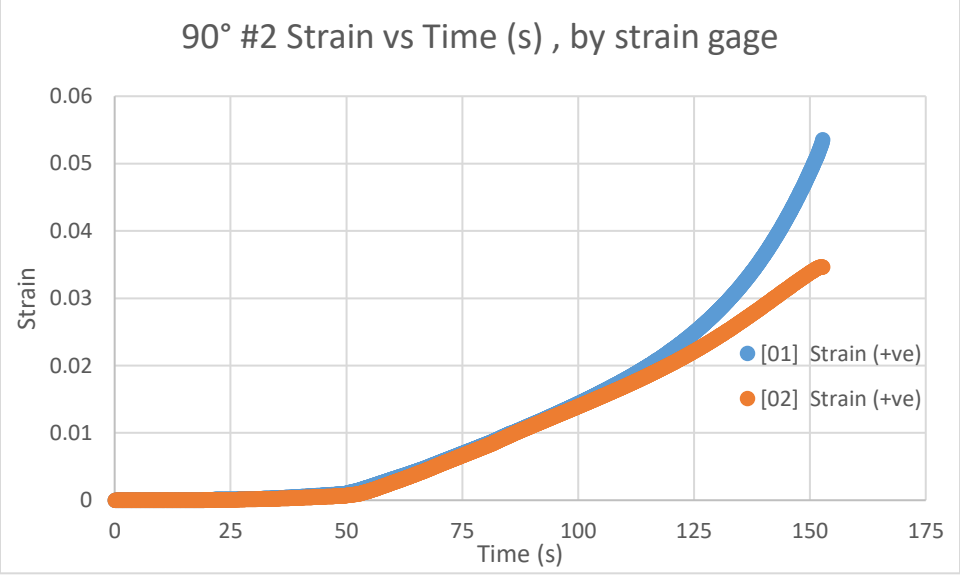

Fig. 39: Strain vs time interval sampling, by strain gage for 90° #2.

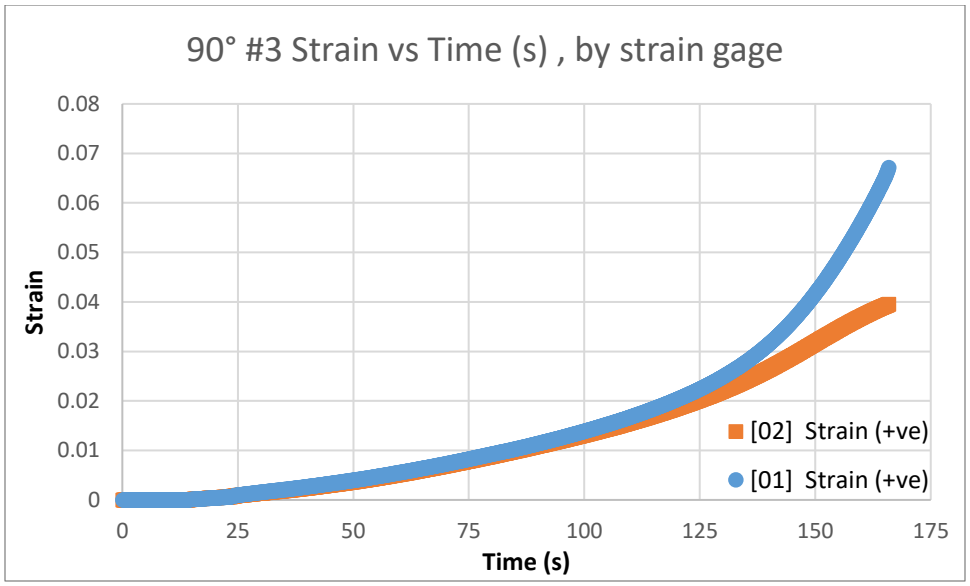

Fig. 40: Strain vs time interval sampling, by strain gage for 90° #3.

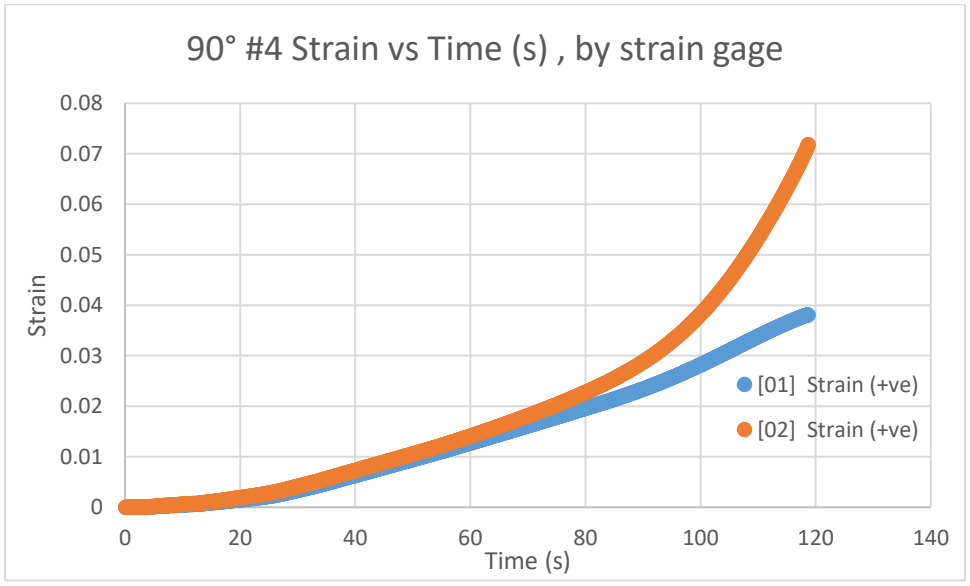

Fig. 41: Strain vs time interval sampling, by strain gage for 90° #4.

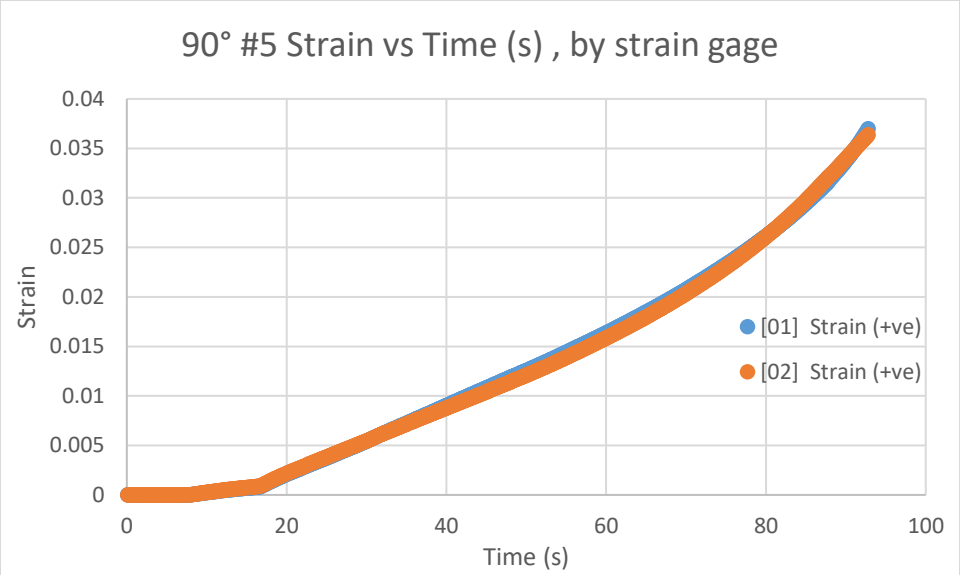

Fig. 42: Strain vs time interval sampling, by strain gage for 90° #5.

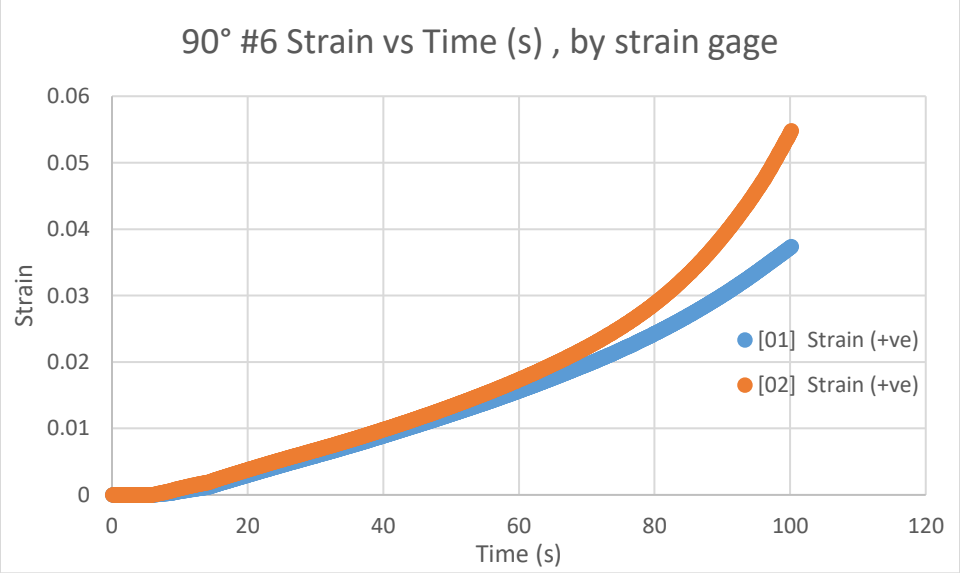

Fig. 43: Strain vs time interval sampling, by strain gage for 90° #6.

Appendix B

Theoretical Predictions

Rule of Mixtures (ROM):

$$E_1 = V_f E_L + (1 - V_f) E_m \quad [1]$$

$$X_1{}^C = G_m/(1 - V_f) \quad [2]$$

$$(E_2)^{-1} = V_f/E_T + (1 - V_f)/E_m \quad [3]$$

A Rule of Mixtures analysis (Equations 1-3) is conducted with consideration to relevant standard deviations. A range of E_1 values will be determined by using Equation 1 ranging by one standard deviation above and below each constituent value to maximize/minimize the resultant E_1 within a standard deviation. E_m is taken as 487ksi, as per the G-83C resin data sheet.[4] Maximum and minimum E_1 values within a standard deviation are calculated below, respectively. E_1 is found to range from 16.26 - 20.21 Msi.

$$E_1 = V_f E_L + (1 - V_f) E_m \quad , \quad E_L = 33.4 \text{ Msi} , E_m = 0.487\text{Msi} , V_f \pm 0.06$$

$$E_1 = V_f(33.4\text{E6}) + (1 - V_f)(0.487\text{E6})$$

$$E_1 = (0.539 + 0.06)(33.4\text{E6}) + \big(1 - (0.539 + 0.06)\big)(0.487\text{E6}) = 20.20\text{Msi}.$$

$$E_1 = (0.539 - 0.06)(33.4\text{E6}) + \big(1 - (0.539 - 0.06)\big)(0.487\text{E6}) = 16.25\text{Msi}.$$

$$E_1 = 16.25 - 20.20 \text{ Msi}.$$

Next, E_2 is calculated in a similar manner, by varying the values of FVF and E_T over their relevant ranges to maximize and minimize the resulting E_2. Maximum and minimum E_2 values within a standard deviation are shown calculated below, respectively. E_2 is found to range from 0.6575 – 0.9983 Msi.

$$(E_2)^{-1} = V_f/E_T + (1 - V_f)/E_m \quad , \quad E_m = 0.487\text{Msi} \text{ , } E_T = 1\text{-}3\text{Msi} \text{ , } V_f \pm 0.06$$

$$(E_2)^{-1} = V_f/E_T + (1 - V_f)/(0.487E6)$$

$$(E_2)^{-1} = (0.539 + 0.06)/(3E6) + (1 - (0.539 + 0.06))/(0.487E6) \rightarrow E_2 = 1.214 \text{ Msi.}$$

$$(E_2)^{-1} = (0.539 - 0.06)/(1E6) + (1 - (0.539 - 0.06))/(0.487E6) \rightarrow E_2 = 0.9347 \text{ Msi.}$$

$$E_2 = 0.9347 - 1.214 \text{ Msi}.$$

Next, X_1^C is found by Equation 2, and similarly maximized and minimized. E_m and ν_m are taken to be 0.487 ksi and 0.351[4], respectively. X_1^C is found to bind the range of 345.94 – 449.47 ksi.

$$X_1^C = G_m/(1 - V_f) \quad , \quad G_m = E_m/(2(1 + \nu_m) \text{ , } E_m = 0.487 \text{ ksi} \text{ , } \nu_m = 0.351 \text{ , } V_f \pm 0.06$$

$$X_1^C = \frac{\left(\frac{0.487E6}{2(1 + 0.351)}\right)}{(1 - 0.599)} = 449,468.5 \text{ psi.} = 449.47 \text{ ksi.}$$

$$X_1^C = \frac{\left(\frac{0.487E6}{2(1 + 0.351)}\right)}{(1 - 0.479)} = 345,944.1 \text{ psi.} = 345.94 \text{ ksi.}$$

Self-Consistent Field Model (CFM):

The given Self-Consistent Field Model spreadsheet was also utilized to predict mechanical properties of the tested compression specimens. Known and manufacturer-provided values were input to the CFM excel spreadsheet, and few outlier unknown variables were left at their as-received value to approximate a typical laminate. The extrema of calculated properties were then ranged by their standard deviation to see their impact on the CFM-predicted properties. The results of these trials are presented below.

Continuous Fiber Micromechanics

Fiber Properties (Transversely Isotropic)	Values	Units	Matrix Properties (Isotropic)	Values	Units
AS4 Graphite			**PEEK**		
Longitudinal Modulus, E1f	3.34E+07	psi	Modulus, Em	4.87E+05	psi
Transverse Modulus, E2f	2.00E+06	psi	Poisson's Ratio, Num	0.351	
Long-Trans Shear Modulus, G12f	7.00E+05	psi	Thermal Exp. Coef., CTE,	1.50E-05	1/F
Trans-Normal Poisson's Ratio, Nu	0.450				
Long-Trans Poisson's Ratio, Nu12	0.320		***Shear Modulus, Gm***	***1.80E+05***	***psi***
Longitudinal CTE, Alpha1f	0.00E+00	1/F			
Transverse CTE, Alpha2f	-3.80E-07	1/F			
			Fiber Volume Fraction, Vf	54%	
Normal Modulus, E3f	***2.00E+06***	***psi***	(Less than 1.0)		
Trans-Normal Shear Modulus	***6.90E+05***	***psi***	***Resin Volume Fractio***	***46%***	
Long-Normal Shear Modulus,	***7.00E+05***	***psi***			
Long-Normal Poisson's Ratio	***0.320***				
Normal CTE, Alpha3f	***#######***	***1/F***			

Predicted Lamina Properties					
Longitudinal Modulus, E1	1.823E+07	psi	Longitudinal CTE, Alpha1	1.900E-07	1/F
Transverse Modulus, E2	9.911E+05	psi	Transverse CTE, Alpha2	8.229E-06	1/F
Normal Modulus, E3	9.911E+05	psi	Normal CTE, Alpha3	8.229E-06	1/F
Trans-Normal Shear Modulus, G23	3.327E+05	psi			
Long-Normal Shear Modulus, G13	3.485E+05	psi			
Long-Trans Shear Modulus, G12	3.485E+05	psi			
Trans-Normal Poisson's Ratio, Nu	0.4895				
Long-Normal Poisson's Ratio, Nu1	0.3330				
Long-Trans Poisson's Ratio, Nu12	0.3330				

Table 10: Nominal values of E2f and FVF

Continuous Fiber Micromechanics

Fiber Properties (Transversely Isotropic)	Values	Units	Matrix Properties (Isotropic)	Values	Units
AS4 Graphite			**PEEK**		
Longitudinal Modulus, E1f	3.34E+07	psi	Modulus, Em	4.87E+05	psi
Transverse Modulus, E2f	1.00E+06	psi	Poisson's Ratio, Num	0.351	
Long-Trans Shear Modulus, G12f	7.00E+05	psi	Thermal Exp. Coef., CTE,	1.50E-05	1/F
Trans-Normal Poisson's Ratio, Nu	0.450				
Long-Trans Poisson's Ratio, Nu12	0.320		***Shear Modulus, Gm***	***1.80E+05***	***psi***
Longitudinal CTE, Alpha1f	0.00E+00	1/F			
Transverse CTE, Alpha2f	-3.80E-07	1/F			
			Fiber Volume Fraction, Vf	48%	
Normal Modulus, E3f	***1.00E+06***	***psi***	(Less than 1.0)		
Trans-Normal Shear Modulus	***3.45E+05***	***psi***	***Resin Volume Fractio***	***52%***	
Long-Normal Shear Modulus,	***7.00E+05***	***psi***			
Long-Normal Poisson's Ratio	***0.320***				
Normal CTE, Alpha3f	***#######***	***1/F***			

Predicted Lamina Properties					
Longitudinal Modulus, E1	1.625E+07	psi	Longitudinal CTE, Alpha1	2.399E-07	1/F
Transverse Modulus, E2	7.215E+05	psi	Transverse CTE, Alpha2	9.879E-06	1/F
Normal Modulus, E3	7.215E+05	psi	Normal CTE, Alpha3	9.879E-06	1/F
Trans-Normal Shear Modulus, G23	2.412E+05	psi			
Long-Normal Shear Modulus, G13	3.224E+05	psi			
Long-Trans Shear Modulus, G12	3.224E+05	psi			
Trans-Normal Poisson's Ratio, Nu	0.4955				
Long-Normal Poisson's Ratio, Nu1	0.3355				
Long-Trans Poisson's Ratio, Nu12	0.3355				

Table 11: Low E2f and low FVF

Continuous Fiber Micromechanics

Fiber Properties (Transversely Isotropic)	Values	Units	Matrix Properties (Isotropic)	Values	Units
AS4 Graphite			**PEEK**		
Longitudinal Modulus, E1f	3.34E+07	psi	Modulus, Em	4.87E+05	psi
Transverse Modulus, E2f	1.00E+06	psi	Poisson's Ratio, Num	0.351	
Long-Trans Shear Modulus, G12f	7.00E+05	psi	Thermal Exp. Coef., CTE,	1.50E-05	1/F
Trans-Normal Poisson's Ratio, Nu	0.450				
Long-Trans Poisson's Ratio, Nu12	0.320		*Shear Modulus, Gm*	*1.80E+05*	*psi*
Longitudinal CTE, Alpha1f	0.00E+00	1/F			
Transverse CTE, Alpha2f	-3.80E-07	1/F			
			Fiber Volume Fraction, Vf (Less than 1.0)	60%	
Normal Modulus, E3f	*1.00E+06*	*psi*	*Resin Volume Fractio*	*40%*	
Trans-Normal Shear Modulus	*3.45E+05*	*psi*			
Long-Normal Shear Modulus,	*7.00E+05*	*psi*			
Long-Normal Poisson's Ratio	*0.320*				
Normal CTE, Alpha3f	*******	*1/F*			

Predicted Lamina Properties					
Longitudinal Modulus, E1	2.020E+07	psi	Longitudinal CTE, Alpha1	1.494E-07	1/F
Transverse Modulus, E2	7.750E+05	psi	Transverse CTE, Alpha2	7.452E-06	1/F
Normal Modulus, E3	7.750E+05	psi	Normal CTE, Alpha3	7.452E-06	1/F
Trans-Normal Shear Modulus, G23	2.607E+05	psi			
Long-Normal Shear Modulus, G13	3.775E+05	psi			
Long-Trans Shear Modulus, G12	3.775E+05	psi			
Trans-Normal Poisson's Ratio, Nu	0.4864				
Long-Normal Poisson's Ratio, Nu1	0.3318				
Long-Trans Poisson's Ratio, Nu12	0.3318				

Table 12: Low E2f and high FVF

Continuous Fiber Micromechanics

Fiber Properties (Transversely Isotropic)	Values	Units	Matrix Properties (Isotropic)	Values	Units
AS4 Graphite			**PEEK**		
Longitudinal Modulus, E1f	3.34E+07	psi	Modulus, Em	4.87E+05	psi
Transverse Modulus, E2f	3.00E+06	psi	Poisson's Ratio, Num	0.351	
Long-Trans Shear Modulus, G12f	7.00E+05	psi	Thermal Exp. Coef., CTE,	1.50E-05	1/F
Trans-Normal Poisson's Ratio, Nu	0.450				
Long-Trans Poisson's Ratio, Nu12	0.320		*Shear Modulus, Gm*	*1.80E+05*	*psi*
Longitudinal CTE, Alpha1f	0.00E+00	1/F			
Transverse CTE, Alpha2f	-3.80E-07	1/F			
			Fiber Volume Fraction, Vf (Less than 1.0)	48%	
Normal Modulus, E3f	*3.00E+06*	*psi*	*Resin Volume Fractio*	*52%*	
Trans-Normal Shear Modulus	*1.03E+06*	*psi*			
Long-Normal Shear Modulus,	*7.00E+05*	*psi*			
Long-Normal Poisson's Ratio	*0.320*				
Normal CTE, Alpha3f	*******	*1/F*			

Predicted Lamina Properties					
Longitudinal Modulus, E1	1.625E+07	psi	Longitudinal CTE, Alpha1	2.402E-07	1/F
Transverse Modulus, E2	1.023E+06	psi	Transverse CTE, Alpha2	9.283E-06	1/F
Normal Modulus, E3	1.023E+06	psi	Normal CTE, Alpha3	9.283E-06	1/F
Trans-Normal Shear Modulus, G23	3.427E+05	psi			
Long-Normal Shear Modulus, G13	3.224E+05	psi			
Long-Trans Shear Modulus, G12	3.224E+05	psi			
Trans-Normal Poisson's Ratio, Nu	0.4917				
Long-Normal Poisson's Ratio, Nu1	0.3346				
Long-Trans Poisson's Ratio, Nu12	0.3346				

Table 13: High E2f and low FVF

Fiber Properties (Transversely Isotropic)	Values	Units	Matrix Properties (Isotropic)	Values	Units
AS4 Graphite			**PEEK**		
Longitudinal Modulus, E1f	3.34E+07	psi	Modulus, Em	4.87E+05	psi
Transverse Modulus, E2f	3.00E+06	psi	Poisson's Ratio, Num	0.351	
Long-Trans Shear Modulus, G12f	7.00E+05	psi	Thermal Exp. Coef., CTE,	1.50E-05	1/F
Trans-Normal Poisson's Ratio, Nu	0.450				
Long-Trans Poisson's Ratio, Nu12	0.320		***Shear Modulus, Gm***	***1.80E+05***	***psi***
Longitudinal CTE, Alpha1f	0.00E+00	1/F			
Transverse CTE, Alpha2f	-3.80E-07	1/F			
			Fiber Volume Fraction, Vf (Less than 1.0)	60%	
Normal Modulus, E3f	***3.00E+06***	***psi***			
Trans-Normal Shear Modulus	***1.03E+06***	***psi***	***Resin Volume Fractio***	***40%***	
Long-Normal Shear Modulus,	***7.00E+05***	***psi***			
Long-Normal Poisson's Ratio	***0.320***				
Normal CTE, Alpha3f	***#######***	***1/F***			

Predicted Lamina Properties					
Longitudinal Modulus, E1	2.020E+07	psi	Longitudinal CTE, Alpha1	1.496E-07	1/F
Transverse Modulus, E2	1.235E+06	psi	Transverse CTE, Alpha2	6.897E-06	1/F
Normal Modulus, E3	1.235E+06	psi	Normal CTE, Alpha3	6.897E-06	1/F
Trans-Normal Shear Modulus, G23	4.162E+05	psi			
Long-Normal Shear Modulus, G13	3.775E+05	psi			
Long-Trans Shear Modulus, G12	3.775E+05	psi			
Trans-Normal Poisson's Ratio, Nu	0.4836				
Long-Normal Poisson's Ratio, Nu1	0.3310				
Long-Trans Poisson's Ratio, Nu12	0.3310				

Table 14: High E2f and high FVF